Title

Long-Term Trends in Seasonality and Abundance of Three Key Zooplankters in the Upper San Francisco Estuary

Journal

San Francisco Estuary and Watershed Science, 21(3)

Authors

Bashevkin, Samuel M.
Burdi, Christina E.
Hartman, Rosemary
et al.

Publication Date

2023

DOI

10.15447/sfews.2023v21iss3art1

Peer reviewed

SAN FRANCISCO ESTUARY & WATERSHED SCIENCE
Sponsored by the Delta Stewardship Council and UC Davis Institute of the Environment

DATA REVIEW

Long-Term Trends in Seasonality and Abundance of Three Key Zooplankters in the Upper San Francisco Estuary

Samuel M. Bashevkin[1*], Christina E. Burdi[2], Rosemary Hartman[3], Arthur Barros[2]

ABSTRACT

Zooplankton provide critical food for threatened and endangered fish species in the San Francisco Estuary (estuary). Reduced food supply has been implicated in the Pelagic Organism Decline of the early 2000s, and further changes in zooplankton abundance, seasonality, and distribution may continue to threaten declining fishes. While we have a wealth of monitoring data, we know little about the abundance trends of many estuary zooplankton species. To fill these gaps, we reviewed past research and then examined trends in seasonality and abundance from 1972 to the present of three key but understudied zooplankton species (*Bosmina longirostris*, *Acanthocyclops* spp., and *Acartiella sinensis*) that play important roles in the estuary food web. We fit Bayesian generalized additive mixed models of each taxon's relationship with salinity, seasonality, year, and geography on an integrated database of zooplankton monitoring in the upper estuary. We found marked changes in the seasonality and overall abundance of each study species. *Bosmina longirostris* no longer peaks in abundance in the fall months, *Acanthocyclops* spp. precipitously declined in all months and lost its strong relationship with salinity, and *A. sinensis* adult abundance has become more strongly related to salinity while juveniles have developed wider seasonal abundance peaks. Through these analyses, we have documented the relationship of each species with salinity and seasonality since the beginning of monitoring or their introduction, thus increasing our understanding of their ecology and importance in the estuary. These results can inform food-web models, be paired with fish data to model the contributions of these species toward fish abundance trends and be mirrored to elucidate other species' trends in future studies.

KEY WORDS

Zooplankton, phenology, salinity, monitoring, generalized additive modeling, copepods, cladocerans, *Bosmina longirostris*, *Acanthocyclops*, *Acartiella sinensis*

SFEWS Volume 21 | Issue 3 | Article 1

https://doi.org/10.15447/sfews.2023v21iss3art1

* Corresponding author: sam.bashevkin@waterboards.ca.gov
Current affiliation: State Water Resources Control Board
Sacramento, CA 95814 USA

1 Delta Science Program
Delta Stewardship Council
Sacramento, CA 95814 USA

2 California Department of Fish and Wildlife
Stockton, CA 95206 USA

3 California Department of Water Resources
West Sacramento, CA 95691 USA

INTRODUCTION

Zooplankton are critical components of aquatic food webs, connecting primary producers to upper trophic species such as fishes. Most fishes rely on zooplankton as a food source during their larval stages when starvation risk is highest (Hunter 1981). The seasonality of fish reproduction is often timed such that larvae coincide with peaks in the abundance of their zooplankton prey (Cushing 1969; Cushing 1990). However, when the seasonality of zooplankton abundance or community composition shifts as a result of climate change, species introductions, or other factors, the starvation risk for larval fishes can increase as their peak abundance no longer coincides with peak food availability (Edwards and Richardson 2004; Durant et al. 2007). Thus, an understanding of the patterns in zooplankton abundance is critical to understanding the drivers of fish abundance.

The San Francisco Estuary (estuary) is home to several fish species listed under the US Endangered Species Act and/or the California Endangered Species Act. Most depend on zooplankton prey for part or all of their life cycle. One of these species, Delta Smelt (*Hypomesus transpacificus*), is endemic to the estuary and relies on zooplankton for its full life cycle (Brown et al. 2016). Another fish, Longfin Smelt (*Spirinchus thaleichthys*), also relies on zooplankton throughout its life cycle (Chigbu and Sibley 1998a; Chigbu and Sibley 1998b; Barros et al. 2022; Lojkovic Burris et al. 2022). A number of fish species, including Delta Smelt and Longfin Smelt, declined sharply in abundance in the early 2000s, during the "pelagic organism decline (POD)" (Feyrer et al. 2007; Sommer et al. 2007). This decline is thought to have been caused in part by reduced zooplankton food supply (Winder and Jassby 2011; Brown et al. 2016; Moyle et al. 2016).

Zooplankton research in the estuary to date has focused on a few key taxa, most notably the copepods *Pseudodiaptomus forbesi*, *Eurytemora affinis*, and *Limnoithona tetraspina*, because they are important food for threatened Delta Smelt and Longfin Smelt (Bouley and Kimmerer 2006; Kimmerer et al. 2014; Kayfetz and Kimmerer 2017; Kimmerer et al. 2018). In floodplains adjacent to the Delta, some cladocerans have also received attention, particularly *Daphnia* spp., because of their importance in the diet of juvenile salmonids (Goertler et al. 2018; Corline et al. 2021).

Many members of the zooplankton community remain under-studied, despite their role in the pelagic food web. One prior study has investigated changes in zooplankton phenology in the estuary. Merz et al. (2016) used a high-level approach to evaluate changes (from 1972 to 2014) to the date of maximum abundance of five zooplankton taxa: *E. affinis*, *Pseudodiaptomus* spp., other calanoids, cyclopoids, and non-copepods. They found that the peak abundances of all these zooplankton groups except the cyclopoids have shifted weeks to months earlier. However, analyses of only the date of peak abundance can overlook the presence of multiple seasonal abundance peaks. Furthermore, the coarse taxonomic resolution of this study excluded analyses of some key species.

In this study, we extensively review prior knowledge and derive new insights from monitoring data in the estuary on three key but understudied zooplankton taxa. We chose to focus on *Bosmina longirostris*, *Acanthocyclops* spp., and *Acartiella sinensis* (Figure 1) because of their importance in estuarine ecology and fish diets (Appendix A) as well as the paucity of prior studies on their dynamics in this estuary. For each taxon, we first review past studies from this estuary and other systems where these taxa occur, then ask three main questions to fill the remaining knowledge gaps: (1) *What is the seasonal abundance pattern?* (2) *What is the relationship of abundance with salinity?* and (3) *How have long-term abundance, seasonal abundance patterns, and salinity relationships changed over time?* To answer these questions, we apply Bayesian generalized additive mixed models to an integrated database of zooplankton monitoring data (Bashevkin et al. 2020; Bashevkin et al. 2022).

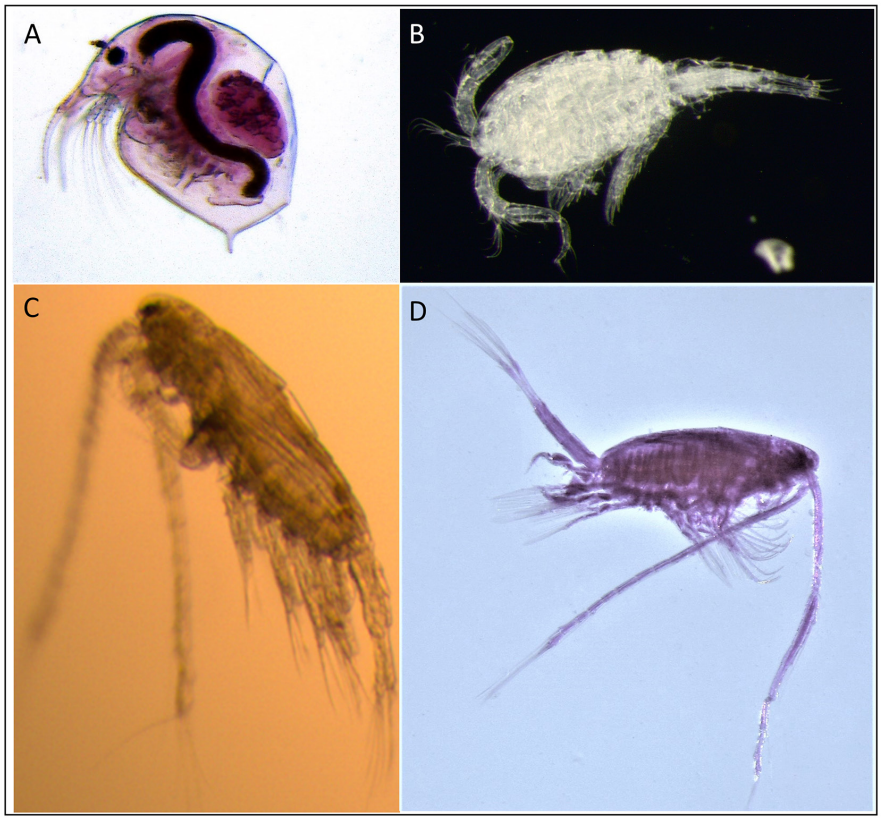

Figure 1 Photographs (*not to scale*) of our study species from the San Francisco Estuary. (**A**) *Bosmina longirostris* adult (approximately 0.3-mm length; credit: CDFW Fish Restoration Program), (**B**) *Acanthocyclops* spp. adult (approximately 1.1-mm length; credit: Tricia Bippus/CDFW), (**C**) *Acartiella sinensis* juvenile male (approximately 1.1-mm length; credit: Anne Slaughter/Estuary & Ocean Science Center, San Francisco State University), (**D**) *Acartiella sinensis* adult male (approximately 1.3-mm length, credit: Michelle Avila/CDFW Fish Restoration Program).

BACKGROUND

Study Area

The San Francisco Estuary (Figure 2) is composed of the tidal, primarily freshwater Sacramento–San Joaquin Delta (Delta), the brackish Suisun Bay, and the more saline San Francisco Bay. This study includes the Delta through the northernmost embayment of San Francisco Bay (San Pablo Bay), since these are the areas with consistent zooplankton monitoring data (hereafter referred to collectively as the upper estuary). The Low-Salinity Zone is an important habitat feature defined by a range of salinities from 0.5 to 2 at the low end, and up to 5 to 6 at the high end. It is an important nursery habitat for fishes such as Delta and Longfin Smelt and moves geographically, depending on outflow levels (and thus seasonally—with higher outflow in winter and spring and lower outflow in summer and fall), ranging between the Carquinez Strait westward and the lower Sacramento and San Joaquin rivers eastward (Hobbs et al. 2006). The Delta receives inflows primarily from the Sacramento River to the north (85%) and the San Joaquin River to the south (11%), with lesser inputs from eastern tributaries: the Cosumnes and Mokelumne rivers (Kimmerer 2002). Almost all inflows come from reservoir releases since very few tributaries are left undammed (Kimmerer 2004; Brown and Bauer 2010). Large export pumps in the South Delta send a portion of these inflows to central and southern California. While annual total inflow and outflow have not changed since the 1950s, inflows have shifted seasonally as reservoir storage has increased in the spring and water releases have increased in the summer (Kimmerer 2002; Hutton et al. 2017).

https://doi.org/10.15447/sfews.2023v21iss3art1

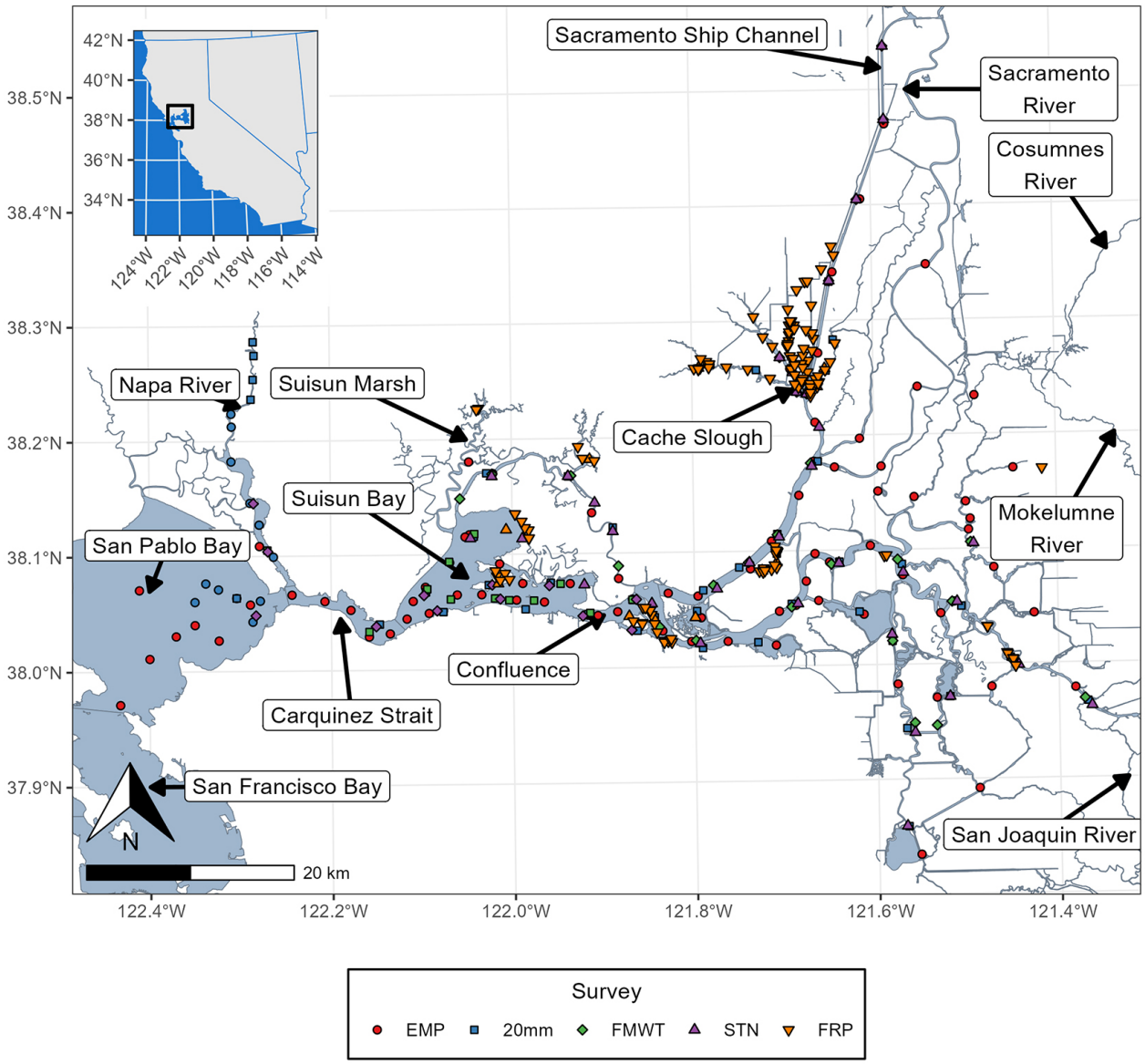

Figure 2 Map of the study area, depicting the sampling stations. Survey abbreviations are as follows: EMP = Environmental Monitoring Program, 20mm = 20-mm Survey, FMWT = Fall Midwater Trawl, STN = Summer Townet, FRP = Fish Restoration Program. The EMP survey has some non-fixed stations that move with the salinity field. Instead of plotting the unfixed stations individually, each is depicted here as the 2.5, 50, and 97.5 percentiles of its in-water distance from the Golden Gate.

Prior Research on the Study Species

Bosmina longirostris

Bosmina longirostris (Figure 1A) is the most abundant cladoceran in the freshwater reaches of the Sacramento–San Joaquin Delta (Bashevkin et al. 2020; Jeffres et al. 2020), where it has been a major component of the zooplankton community over the past 40 years (Ambler et al. 1985). Like *Daphnia* spp., it is abundant in off-channel habitat in the estuary (Corline et al. 2021), but unlike *Daphnia* spp., it is also abundant in the larger channels of the South Delta (Bashevkin et al. 2020; Jeffres et al. 2020). *Bosmina* spp. are consumed by fishes including juvenile salmonids and juvenile and adult Delta Smelt (Appendix A) (Roegner et al. 2015; Goertler et al. 2018; Slater et al. 2019), but they rarely occur in the diets of larval Longfin

Smelt (Appendix A) (Jungbluth et al. 2021; Lojkovic Burris et al. 2022), likely because of a mismatch in the optimal salinities of *Bosmina* spp. and Longfin Smelt. Their small size makes them generally less consumed than larger *Daphnia* spp. by juvenile salmon (Craddock et al. 1976; Holm and Møller 1984). In a Swedish lake, juvenile perch with diets that contained high percentages of *Bosmina* spp. grew more slowly (Romare 2000). Both *Daphnia* spp. and *Bosmina* spp. tend to have lower nutritional quality (as measured by fatty acids) than copepods (Kratina and Winder 2015).

Bosmina longirostris is a small, filter-feeding cladoceran found in lakes and rivers throughout the world. Despite its widespread occurrence, its ecology has received little attention because of its small body size and complicated taxonomy (Adamczuk 2016). Despite its small size in comparison to members of the better-studied genus *Daphnia*, *B. longirostris* can still affect the food web. *Bosmina longirostris* is particularly effective in depressing biomass of small phytoplankton (Carpenter and Kitchell 1984) and is an efficient consumer of ciliates and bacteria (Jürgens et al. 1996), thus playing a key role in the microbial loop. *Bosmina longirostris* feeds broadly on phytoplankton, protists, and bacteria, but exhibits positive selection for larger algal cells (1 to 15 µm) over smaller bacterial cells (< 1 µm) (Balcer et al. 1984; Onandia et al. 2015). It can also thrive on many types of cyanobacteria (Tõnno et al. 2016). *Bosmina longirostris* tolerates disturbance more than many species of *Daphnia* (Hart 2004; Adamczuk 2016), with greater resistance to toxic cyanobacteria (Matveev and Balseiro 1990; Jiang et al. 2013; Jiang et al. 2014; Jiang et al. 2017), and a higher salinity tolerance than many other cladocerans (Adamczuk 2016). *Bosmina* spp. also have a higher thermal tolerance than many freshwater zooplankton (Drenner et al. 1981; Jiang et al. 2014), leading to the potential for their increasing advantage over other zooplankton as temperatures rise. *Bosmina longirostris* typically lives 20 to 50 days and reproduces parthenogenically, producing two to six broods of two to four embryos each, though temperature, salinity, and predation may affect lifespan and reproduction (Adamczuk and Mieczan 2019).

Acanthocyclops spp.

Acanthocyclops spp. (Figure 1B) is a cyclopoid of unknown origin which occurs mostly in freshwater (Orsi and Mecum 1986). Previous studies in the estuary identified the species of *Acanthocyclops* in this region as *Acanthocyclops vernalis;* however, research in other systems discovered that *A. vernalis* is a species complex consisting of three cryptic species; *Acanthocyclops robustus*, *Acanthocyclops americanus*, and *A. vernalis* (Alekseev et al. 2002; Dodson et al. 2003; Miracle et al. 2013; Alekseev 2021). Because these are difficult to distinguish by morphology, it is not known whether all three species in the *A. vernalis* complex are native to the estuary or were introduced at some point in the past; however, Jungbluth et al. (2021) did find molecular evidence of all these species in larval Longfin Smelt diets collected in this region in 2017.

Before the introduction of the small cyclopoid *L. tetraspina* in 1993 (Orsi and Ohtsuka 1999), *Acanthocyclops* spp. was the most abundant cyclopoid in the estuary (Orsi and Mecum 1986). *Acanthocyclops* spp. is an important component of fish diets in this region, particularly for Longfin Smelt (see Appendix A; Hobbs et al. 2006; Lojkovic Burris et al. 2022) and larval Pacific Herring (*Clupea pallasii*) (Jungbluth et al. 2021), with *Acanthocyclops* spp. being the most abundant cyclopoid detected in larval Longfin Smelt gut contents by molecular sequencing (Jungbluth et al. 2021). *Acanthocyclops* spp. also has a higher nutritional value than *L. tetraspina*, and a similar fatty acid composition to that of the calanoid copepods *E. affinis* and *P. forbesi* (Kratina and Winder 2015).

While research on the ecology and biology of *Acanthocyclops* spp. is relatively limited in the estuary, the *A. vernalis* complex has been studied extensively in other freshwater and estuarine systems in Europe, Russia, and the Great Lakes. Studies in these systems show that, despite the morphological similarities, *A. vernalis*, *A. robustus*, and *A. americanus* have

https://doi.org/10.15447/sfews.2023v21iss3art1

different ecologies, life cycles, and environmental tolerances (Alekseev et al. 2002; Miracle et al. 2013; Alekseev 2021). *Acanthocyclops vernalis* and *A. robustus* inhabit freshwater littoral or near-benthic areas, and *A. vernalis* has a benthic naupliar stage (Alekseev et al. 2002; Miracle et al. 2013). Adult and juvenile *A. vernalis* also were found to vertically migrate from the bottom into the water column at night (Evans and Stewart 1977). Both *A. vernalis* and *A. robustus* are predominantly predatory, consuming copepod nauplii, cladocerans, rotifers, and occasionally larval fishes (Anderson 1970; Kerfoot 1978; Gliwicz and Stibor 1993; Piasecki 2000). By contrast, *A. americanus* is pelagic throughout its life cycle, has been found in salinities from the Mediterranean Sea (Alekseev 2021) to freshwater lakes (Alekseev et al. 2002), and is omnivorous. *Acanthocyclops americanus* nauplii consume algae primarily, with later life stages also consuming filamentous algae and cyanobacteria, in addition to cladocerans, nauplii, and rotifers (Enríquez–García et al. 2013; Sarma et al. 2019). All species can produce about 100 eggs per female, develop to sexual maturity in 10 to 14 days, and live 30 to 75 days depending on conditions, with *A. americanus* growing and reaching maturity faster than the other species (Alekseev 2021). Species in the *A. vernalis* complex likely have different environmental tolerances, as has been shown by studies of their seasonal and spatial variation in abundance in other regions. *Acanthocyclops vernalis* may tolerate colder temperatures more than the other species, whereas *A. americanus* could tolerate higher temperatures based on laboratory experiments and timing of peak abundance in areas outside the estuary (Alekseev 2021).

Acartiella sinensis

In the fall of 1993, the non-native calanoid copepod *A. sinensis* (Figure 1C and 1D) was first detected in the estuary (Orsi and Ohtsuka 1999). Likely introduced via the ballast water of ships, the large (~1.2 to 1.5 mm in length) predatory calanoid is native to Southeast Asia (Shen and Lee 1963; Srinui and Ohtsuka 2015). The species has been recorded from estuaries along the East China Sea in salinities around 18 to 21 (Shen and Lee 1963) to the brackish marshes of Thailand in salinities around 5 and average water temperatures around 31 °C (Srinui and Ohtsuka 2015). In the Pearl River estuary of China, *A. sinensis* was the dominant copepod in brackish waters with salinities less than 15 (Tan et al. 2004). Sampling in the Thale–Noi Lake of Thailand showed that changes in temperature and salinity were the main environmental variables that affected densities of *A. sinensis* in the region (Inpang 2008).

Within a year after introduction, *A. sinensis* became the second most common calanoid copepod in the upper estuary, with its highest abundances in the Low-Salinity Zone during summer and fall (Hennessy 2018). *Acartiella sinensis* is predatory and has been shown to feed on copepod nauplii and copepodids, primarily *L. tetraspina* and *P. forbesi* (York et al. 2014; Slaughter et al. 2016; Kayfetz and Kimmerer 2017). *Acartiella sinensis* is also a common food item for the endangered Delta Smelt as well as the more abundant American Shad (Appendix A), mostly in summer and fall (Slater and Baxter 2014; Slater et al. 2019).

Since the introduction of *A. sinensis* in 1993, the zooplankton assemblage in the low-salinity Suisun area has shifted in trophic composition. Once dominated by herbivorous cladocerans and copepods such as *E. affinis* and *P. forbesi*, the community has become more "top-heavy" with the spread of *A. sinensis* (Kratina et al. 2014; Kratina and Winder 2015). The sustained prevalence of *A. sinensis* in the Low-Salinity Zone and its high predation rate on the nauplii of *P. forbesi* are linked to a shift in the spatial distribution of *P. forbesi* out of the Low-Salinity Zone and upriver into more freshwater habitats (Kayfetz and Kimmerer 2017). This shift in *P. forbesi* distribution could have implications for most planktivorous fishes that feed on the calanoid copepod populations.

MATERIALS AND METHODS

Zooplankton Data

The data used for these analyses were obtained from an integrated database of five long-term

zooplankton monitoring surveys in the upper estuary: The Environmental Monitoring Program (EMP), 20-mm Survey (20-mm), Fall Midwater Trawl (FMWT), Summer Townet (STN), and Fish Restoration Program monitoring (FRP). These surveys are described in detail in Kayfetz et al. (2020) and Bashevkin et al. (2022). Briefly, EMP samples monthly year-round since 1972, 20-mm samples every other week March through July since 1995, STN samples every other week from June through August since 2005, FWMT samples monthly September through December since 2011, and FRP samples annually or monthly near tidal marshes (or areas soon to be restored to tidal marshes) March through December since 2015. Each survey samples at a set of fixed stations (Figure 2). EMP also samples at a set of moving stations at locations where the bottom conductivity is 2 and 6 mS cm^{-1}. Many of these surveys collect other parameters such as fish abundance or water quality, but only the time-period of zooplankton sampling is described above. Furthermore, sampling locations and frequencies have changed over time (Kayfetz et al. 2020; Bashevkin et al. 2022).

The data from each survey are integrated by the R package zooper (Bashevkin 2021), which imports and standardizes the data from each survey. Zooplankton abundances are reported as the number of organisms m^{-3}, but these abundances are derived from counts of sub-samples. Information on the sub-sampling approaches can be found in Bashevkin et al. (2022). For these analyses, we selected data from the mesozooplankton size-class, which corresponds to samples from the modified Clarke–Bumpus nets used by each survey, with mesh sizes of 150 (FRP) to 160 (all surveys except FRP) µm. We selected all available data from each of our study species without missing values in our covariates. When possible, adults and juveniles were analyzed separately since these distinct life stages have different behaviors and abundance drivers and play distinct demographic roles. *Acartiella sinensis* was introduced to the estuary in 1993 (Orsi and Ohtsuka 1999), but adults were first counted in samples in 1994 and juveniles were first counted in 2006. Thus, adult data were filtered to the start date of 1994 and juveniles to the start date of 2006. For the other species, only adult data were available at the taxonomic resolution of our analysis. The final data set had 33,255 samples for *B. longirostris* adults, 32,026 samples for *Acanthocyclops* spp. adults, 17,189 samples for *A. sinensis* adults, and 11,224 samples for *A. sinensis* juveniles.

Exploratory data visualization revealed tighter relationships of each species' abundance with log-transformed salinity than raw salinity values. Thus, salinity was natural log-transformed for analyses. Furthermore, we standardized all covariates (including log-transformed salinity) by subtracting the mean and dividing by the standard deviation. Lastly, since many of the sampling stations from the different surveys were near one another (Figure 2), we clustered all stations into groups (hereafter referred to as "station clusters") within a 1-km radius.

Model Structure

We fit Bayesian generalized additive mixed models with the R package brms (Bürkner 2017; Bürkner 2018), which uses the Bayesian modeling platform Stan (Stan Development Team 2021), as well as the R package mgcv (Wood 2011) to construct the generalized additive model smooths. Smooths enable the modeling of non-linear relationships of arbitrary shape; they make no assumptions about the shape of the curve. They can thus be used to model unimodal curves such as the relationship between salinity and abundance, multimodal curves such as interannual trends in abundance, and cyclical curves such as seasonal patterns. Smooths are constructed with different types or combinations of splines, which produce the modeled curves. Splines are smooth functions constructed from a number of component basis functions. The "wiggliness" of the spline is controlled by the basis dimension (k), which controls the maximum number of basis functions in the spline. Thus, splines with higher basis dimensions are allowed to produce more wiggly curve shapes, while splines with lower basis dimensions are constrained to smoother curve shapes. Similar to interactions among effects in linear models,

https://doi.org/10.15447/sfews.2023v21iss3art1

splines can also interact with one another. In this case, spline interactions produce a multi-dimensional smoothed surface in which the interactions themselves are also nonlinear, rather than the single curves that would be produced without interactions.

Models were fit with a hurdle lognormal distribution, using the abundance (organisms m^{-3}) of the specified taxon and life stage as the response variable. Models were fit to the raw sample-level data, not to data aggregated to the level of the station clusters. Hurdle models account for excessive zeros in the response by separately modeling the probability of absence (0 abundance, referred to as the hurdle probability) and the probability of the non-zero values (i.e., abundance, given presence).

We initially explored a wide range of model structures on the *B. longirostris* data to determine the structure that best fits the data and best addresses our questions. To explore different methods of accounting for spatial effects, we created a matrix of the in-water distance between all possible pairs of sampling stations. We then used this matrix to evaluate whether models with the covariance matrix of the random intercepts for each station cluster constrained to this distance matrix would be superior to models with simple random intercepts for each station cluster. We also evaluated models with polynomials instead of splines, year and salinity coded as categories or continuous metrics, different combinations of our predictors, and the hurdle probability modeled with a simple intercept or an effect of salinity. Model fit was evaluated for each option (see below) and compared to one another with leave-one-out (LOO) cross-validation using the R package loo (Vehtari et al. 2017). LOO cross-validation estimates the out-of-sample prediction accuracy of the model and can estimate an information criterion to compare model fits. We did not evaluate models with different basis dimensions (wiggliness parameters) since those values were determined a priori based on the resolution at which we wanted to model the data (see justifications below) and our understanding of the data-collection methods and species cycles (e.g., it would not have made sense to attempt to model daily seasonality when most surveys collect data monthly). Furthermore, increasing the basis dimensions above the values we chose would have resulted in computationally infeasible models since the number of parameters would have vastly increased. We selected the final model structure among those with good fit metrics as the best combination of parsimony and LOO cross-validation information criteria (i.e., it had the best—lowest—LOO information criterion or equivalent criterion to more complex structures).

Our overall approach in the final model structure was to model the probability of presence with a smoothed function of salinity, and the non-zero abundances with smooth functions of day of year, salinity, year, and their interactions, while accounting for space with a random intercept for each station cluster. Our combination of a Bayesian method, which propagates uncertainty and handles unbalanced data, with a generalized additive model approach, which accounts for key covariates like salinity and seasonality, allowed us to resolve inconsistencies in the sampling designs, and incorporate samples from both fixed stations and stations that move with the salinity field.

The hurdle probability (probability of 0 abundance) was modeled with a cubic regression spline of salinity with a low basis dimension (k) of 5 since the relationship was expected to have a simple unimodal shape. The abundance of *Acartiella sinensis* was so strongly seasonal that we modified the hurdle component to also include seasonality. Thus, for *A. sinensis* we modeled the hurdle probability with a two-dimensional (2-D) tensor product smooth (i.e., an interaction) of salinity (cubic regression spline, k=5) and day of year (cyclic cubic regression spline, k=4). The basis dimension for day of year was also set low because we similarly expected a simple shape of the relationship with absence probability.

The non-zero abundances were modeled with a 3-D tensor product smooth (i.e., an interaction) of day of year (cyclic cubic regression spline, k=13), salinity (cubic regression spline, k=5), and year (cubic regression spline, k=5). The basis

dimension for day of year was set to 13 to match the monthly interval of these sampling programs (a basis dimension of 13 has 12 independent functions). The basis dimension for salinity was set to the lower value of 5 because the relationship with salinity was expected to be a simple unimodal shape, and a basis dimension of 5 would still allow much greater complexity than a simple unimodal shape. The basis dimension for year was set to the low value of 5 because we were interested in evaluating broad long-term patterns, rather than fine-scaled, year-to-year abundance trends. Thus, the results of this model represent broad long-term trends, not predicted abundances for specific years. For juvenile *A. sinensis,* the basis dimension for year was reduced to 3 since they have been counted in samples only since 2006 and thus the time-series is shorter. We also included a random intercept for each station cluster.

We fit separate models on each species and life stage (four total). Models were run on three chains, each for 5,000 iterations, including 1,250 used for the warm-up that were then discarded. We used weakly informative priors as recommended by the Stan authors (Stan Development Team 2021). These priors aid model fitting by providing more probability to more reasonable parameter values but are weak enough to be overwhelmed by a reasonable amount of data. Our priors were as follows for each parameter type:

- **Abundance intercepts:** Normal distribution with mean 0 and standard deviation 10
- **Hurdle intercepts:** Logistic distribution with location 0 and scale 1
- **Slopes:** Normal distribution with mean 0 and standard deviation 5
- **Random intercept standard deviations:** Half-Cauchy distribution with location 0 and scale 5
- **Spline standard deviation:** Student t distribution with 3 degrees of freedom, mean 0, and scale 4.7

We validated and checked each model prior to use. We inspected all models to ensure adequate sampling by verifying the posterior effective sample size (> 100 per chain) and Rhat values (< 1.05) (McElreath 2015). We further inspected visual plots, comparing the model outputs to the raw data to ensure they matched. These plots included the proportion of zero values, the distribution of non-zero abundance values, and the predicted non-zero abundance values for each row in the data set. We also inspected the spatio-temporal variograms for spatio-temporal auto-correlation using the R package gstat (Pebesma 2004; Gräler et al. 2016). We detected some residual auto-correlation, and thus used a conservative 99% credible interval when plotting the model results to account for any potential effects.

Model Predictions

We visualized predicted values from the models to explore the abundance patterns of each species and life stage. We generated predicted values over a range of covariates that included all combinations of six evenly spaced time-points per month (from 1972 to 2019) and a series of salinity values selected as quantiles from the raw data (every 0.05 from 0.05 to 0.95). With this approach, each salinity quantile represents the boundary of a salinity bin, and every salinity bin contains an equal number of samples. Since there were some gaps in the time-series (e.g., winters were not sampled some years in the 1970s and 1980s), those same gaps are preserved in the model predictions to avoid extrapolation. We then plotted model predictions along with their 99% credible intervals. To visualize the multi-dimensional model outputs, we created three plots for each set of model predictions. Each plot had one of the covariates (salinity, day of year, or year) on the *x*-axis while the other two variables were illustrated with color or separate plots. For the two covariates included as color or separate plots, we chose a subset of the previously selected quantiles used in generating model predictions to reduce plot complexity and aid interpretation. We chose these values as an evenly spaced subset of the values available. For example, for plots with salinity on the color scale, we chose salinity

https://doi.org/10.15447/sfews.2023v21iss3art1

quantiles of 0.05, 0.35, 0.65, and 0.95, (i.e., the four evenly spaced quantiles along the range we used).

To explore spatial patterns in abundance, we extracted the mean estimated value from each station cluster random intercept. We then plotted these values over a map of the study region. The code used in these analyses is available at *https://github.com/sbashevkin/SDP*.

RESULTS

Bosmina longirostris Adults

The abundance of adult *B. longirostris* has regularly peaked in the spring between April and May (Figure 3). In earlier years, another large peak occurred in the late summer to fall between August and October. In some years (1980 and 1985), this fall peak was as large as the spring peak. However, by 1990, the fall peak was greatly reduced to just a small increase, which has since continued to decrease in size, becoming non-existent by 2015.

Bosmina longirostris adults were most abundant in freshwater, and abundance decreased as salinity increased (Figure B1). In the second-highest salinity bin (1.113), the fall peak was larger than the spring peak in earlier years. However, the fall peak at this and lower salinities was greatly reduced by 1995, shrinking smaller than the spring peak even as the overall abundance in this salinity continued to decrease over time (Figures 3 and B1).

The abundance of adult *B. longirostris* has declined in most months (Figure 4). This is most apparent in August through November, corresponding to the loss of their former fall peak. In some months, their abundance has mostly decreased over time, except in recent years, which have a slight uptick. This recent uptick appears in January through March and May through July but is largest in May through July.

Controlling for all other factors (salinity, year, month), *B. longirostris* adult abundance was highest in the southeastern Delta (Figure 5). Other areas near the boundaries of the sampled area also had higher abundances such as in San Pablo Bay, Napa River, and parts of the Cache Slough Complex and Sacramento Deep Water Ship Channel. The Sacramento River corridor between Cache Slough and Suisun Bay generally had low abundance, as did parts of the northeastern Delta.

Acanthocyclops spp. Adults

The abundance of *Acanthocyclops* spp. adults has peaked regularly in the spring from April to May in all years (Figure 6). This peak was apparent in the two lower salinity bins (0.062 and 0.137) but generally not in the two higher salinity bins (1.402 and 13.017). In the second-highest salinity bin (1.402), abundance peaked in the winter from February through March in most years, although limited sampling in these months in some years may have masked the signal.

In the earlier years (before ~2000), *Acanthocyclops* spp. were most abundant in the lower salinities, peaking around 0.3 (Figure B2). Abundance decreased on either side of that peak but fell much lower in the highest salinities. Over the years, the relationship of *Acanthocyclops* spp. with salinity in October through February leveled out such that they became equally abundant in all salinity levels up to 3.

The abundance of *Acanthocyclops* spp. has precipitously declined over time in all months (Figure 7). There was a slight uptick in the 1980s to 1990s in most months, but populations crashed again after this period. Overall trends in January and February were mostly flat with generally low abundance in all years, but the missing data in those months may be obscuring patterns.

The highest *Acanthocyclops* spp. abundance after controlling for the other covariates was in Cache Slough, Suisun Marsh, the southeastern Delta, Carquinez Strait, San Pablo Bay, and the Napa River (Figure 8). The lower Sacramento and San Joaquin rivers through Suisun Bay generally had lower abundances, as did most of the western-most areas.

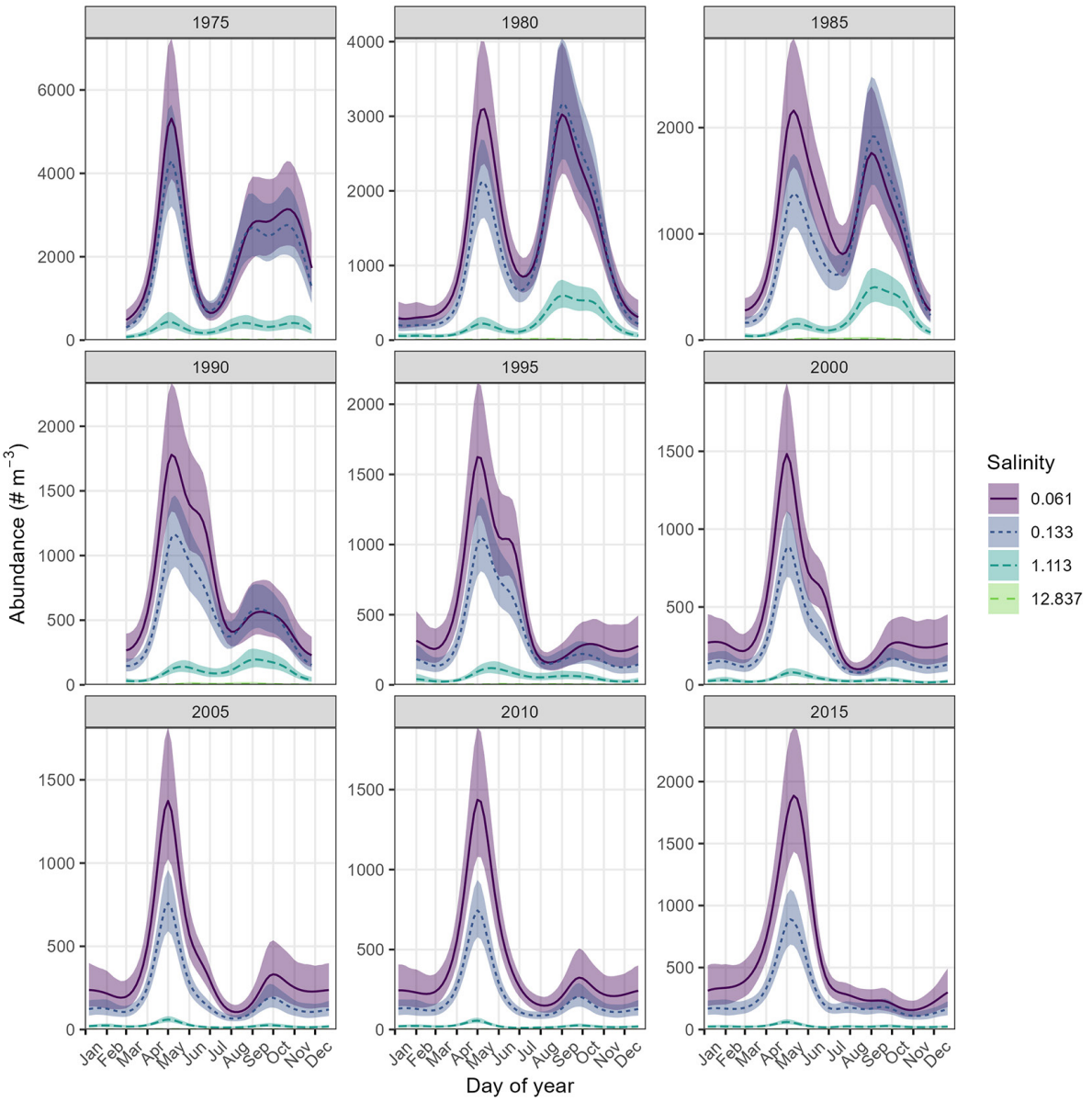

Figure 3 Seasonal patterns in *Bosmina longirostris* adult abundance with 99% credible intervals. Each plot represents predictions from a different position on the smoothed yearly trend, which was restricted in its "wiggliness" to favor capturing the long-term trends over year-to-year swings in abundance. Thus, the plots for each year may not represent exact conditions for that year, but rather the average abundance for a few years before through a few years after the year portrayed. Predictions for different salinity values are represented by *line* and *shading color*, as well as *line type*. The *y*-axis limits differ among plots to facilitate comparison of seasonal trends. Absolute trends in abundance over time are represented in Figure 4. Missing values (e.g., the months of Jan, Feb, and Dec in 1975) represent gaps in the raw data. Salinity is reported on the Practical Salinity Scale.

***Acartiella sinensis* Adults**

Acartiella sinensis had the strongest seasonality of the three species investigated. Adults peaked in the fall from August through December, with the highest levels in September and October (Figure 9). Abundances then dipped close to zero from February through May.

Adult *A. sinensis* were most abundant in salinities between about 1 and 4 (Figure B3). The effect of salinity on abundance has increased over time,

https://doi.org/10.15447/sfews.2023v21iss3art1

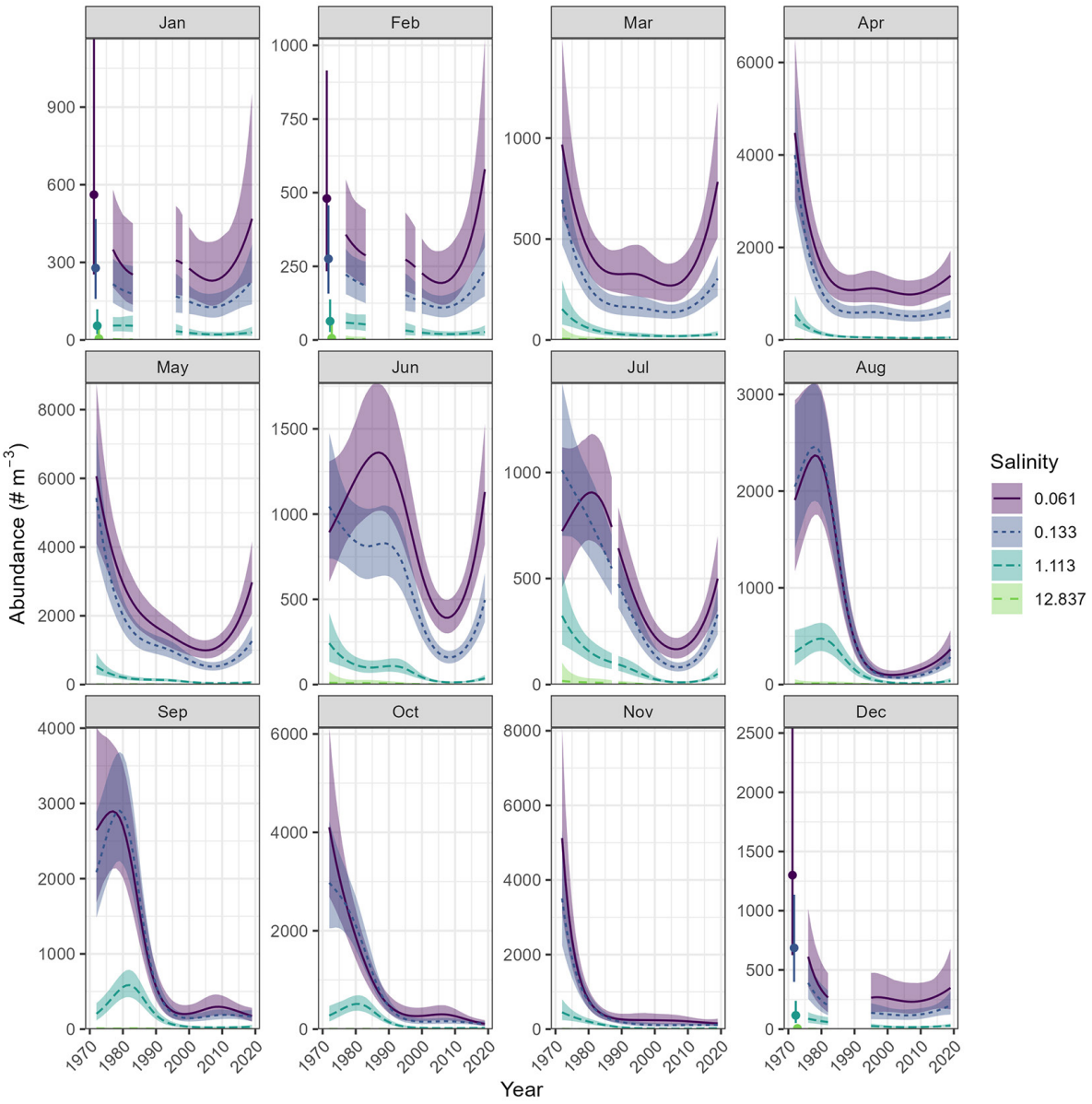

Figure 4 Yearly patterns in *Bosmina longirostris* adult abundance with 99% credible intervals. Each plot represents the pattern for a separate month. Predictions for different salinity values are represented by line and shading color, as well as line type. The *y*-axis limits differ among plots to facilitate comparison of long-term trends. Seasonal trends in abundance are represented in Figure 3. Missing values represent gaps in the raw data. Salinity is reported on the Practical Salinity Scale.

especially in May through July where the peak was greatly reduced in earlier years.

Unlike the other two species, *A. sinensis* adults did not exhibit any overall long-term decreases in abundance (Figure 10). However, the time-series was shorter, only starting in 1994. In most months, the most recent abundance was similar to the earliest abundance level, but abundance did increase over time in March through July. The abundance peaked in the 2010s in most months, and some months also had an earlier peak around 2000.

Spatially, *A. sinensis* adult abundance was highest (controlling for all other covariates) along the

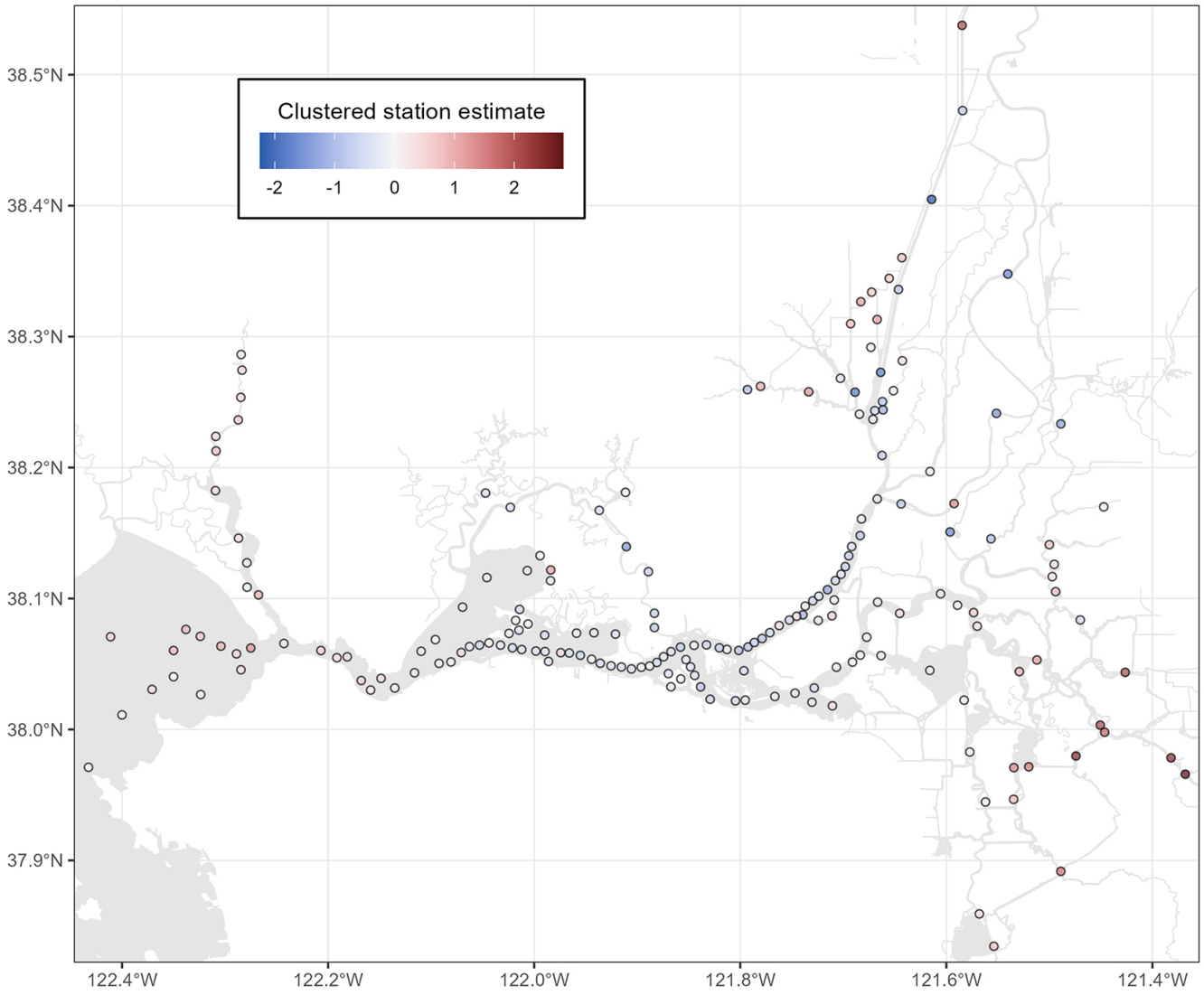

Figure 5 Estimated values of the random intercepts for station clusters in the *Bosmina longirostris* adult model. Stations within 1 km were clustered into station clusters, plotted here as separate points. *Point color* indicates whether each station cluster has higher or lower *B. longirostris* adult abundance, after controlling for the other covariates (day of year, salinity, and year).

corridor from the lower Sacramento River just below Cache Slough all the way through to Carquinez Strait (Figure 11). The southeastern and northern Delta had the lowest abundances.

Acartiella sinensis Juveniles

Like the adults, juvenile *A. sinensis* also had strong seasonal abundance patterns, peaking over just a few months and then subsiding to close to 0 abundance (Figure 12). Peaks occurred in the summer from July through September, but the width of the seasonal peak grew over time. Around 2006 they were abundant for just 2 months (July and August), while from about 2015 to 2018 they were abundant from April through November.

Acartiella sinensis juveniles were abundant in higher salinities > 4 but declined at the very highest salinities close to 16 (Figure 12). Their abundance in lower salinities increased over time but always remained lower than their abundance at the higher salinities (Figure B4). In most years, the seasonal abundance peak was 1 to 2 months

https://doi.org/10.15447/sfews.2023v21iss3art1

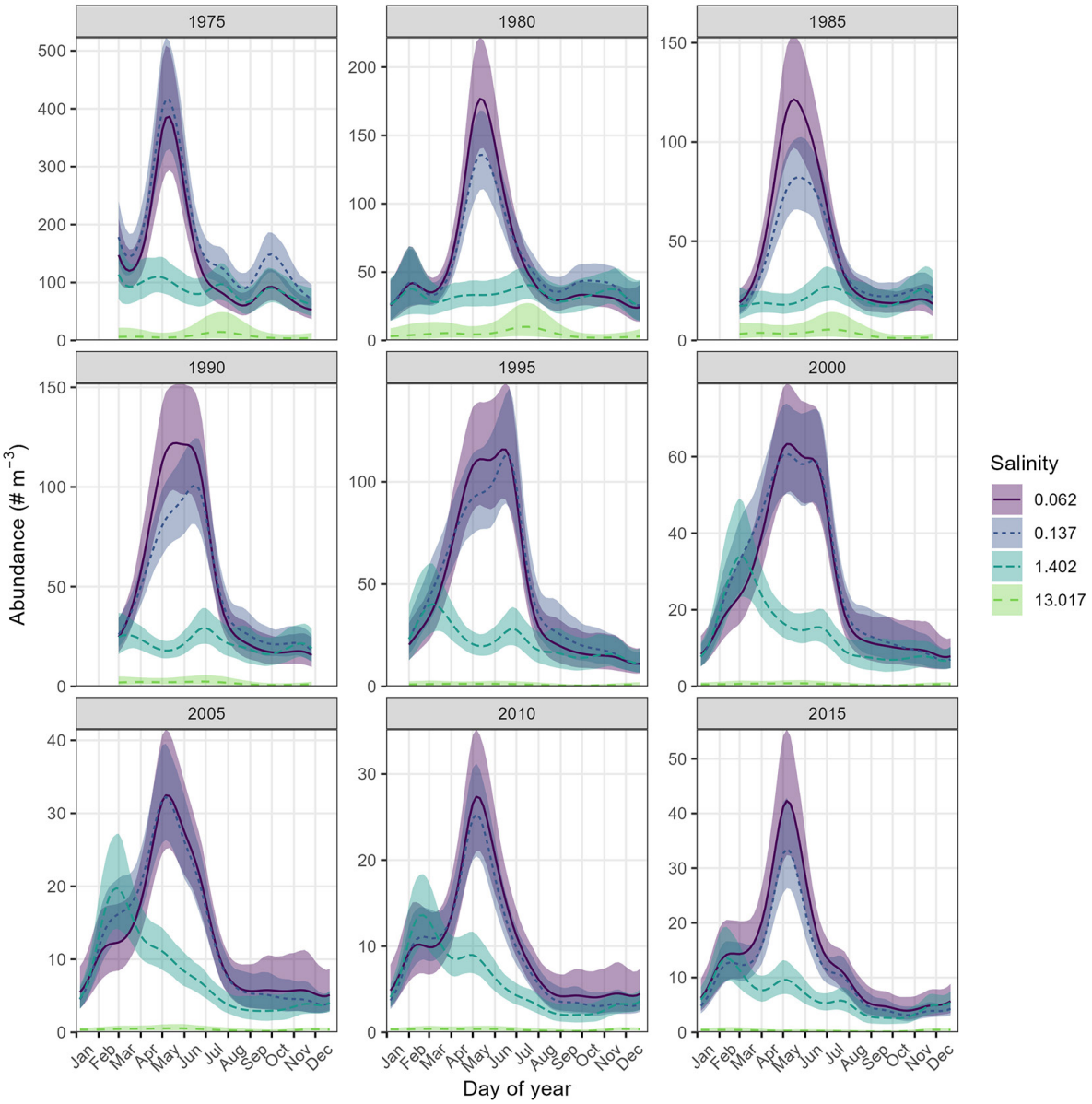

Figure 6 Seasonal patterns in *Acanthocyclops* spp. adult abundance with 99% credible intervals. See Figure 3 for a full description.

later at the highest salinity of ~16 than the other salinity levels.

While the time-series was much shorter (2006 through 2020) for *A. sinensis* juveniles than for any of the other species and life stages investigated, we did detect some long-term trends in some months (Figure 13). The trends were most apparent in the second-highest salinity of 2.703 where *A. sinensis* juveniles were most abundant. Abundance increased over the years in April through June and decreased in August. This corresponds to the widening of the seasonal peak over time. The other months generally did not have any long-term trends.

The spatial pattern of *A. sinensis* juveniles was less clear than those of the other species and life stages (Figure 14). However, they were generally most abundant along the San Joaquin River corridor in the southern Delta and in some Suisun Bay station clusters. They were least abundant

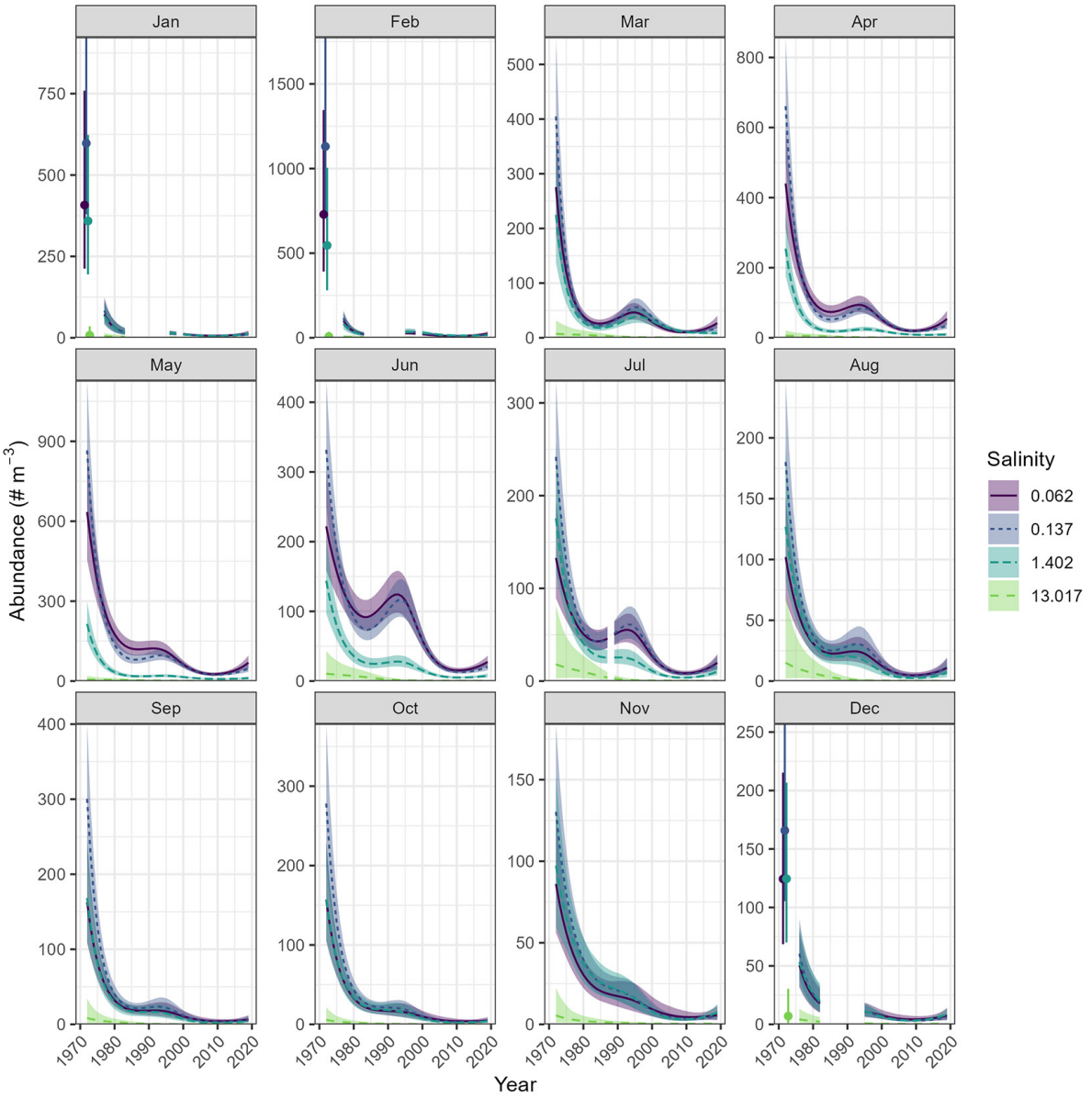

Figure 7 Yearly patterns in *Acanthocyclops* spp. adult abundance with 99% credible intervals. See Figure 4 for a full description.

in the lower Sacramento River between Cache Slough and the confluence of the Sacramento and San Joaquin rivers, as well as in the Napa River and eastern Suisun Marsh.

DISCUSSION

We found marked changes in the seasonality and overall abundance of three key zooplankton taxa in the upper estuary. *Bosmina longirostris* no longer peaks in abundance in the fall months, *Acanthocyclops* spp. precipitously declined and lost its strong relationship with salinity in most months, and *A. sinensis* adult abundance has become more strongly related to salinity while juveniles have developed wider abundance peaks. In this process, we have documented the relationship of each species with salinity and seasonality back to the beginning of monitoring or their introduction, increasing our understanding of their ecology and importance in the estuary.

https://doi.org/10.15447/sfews.2023v21iss3art1

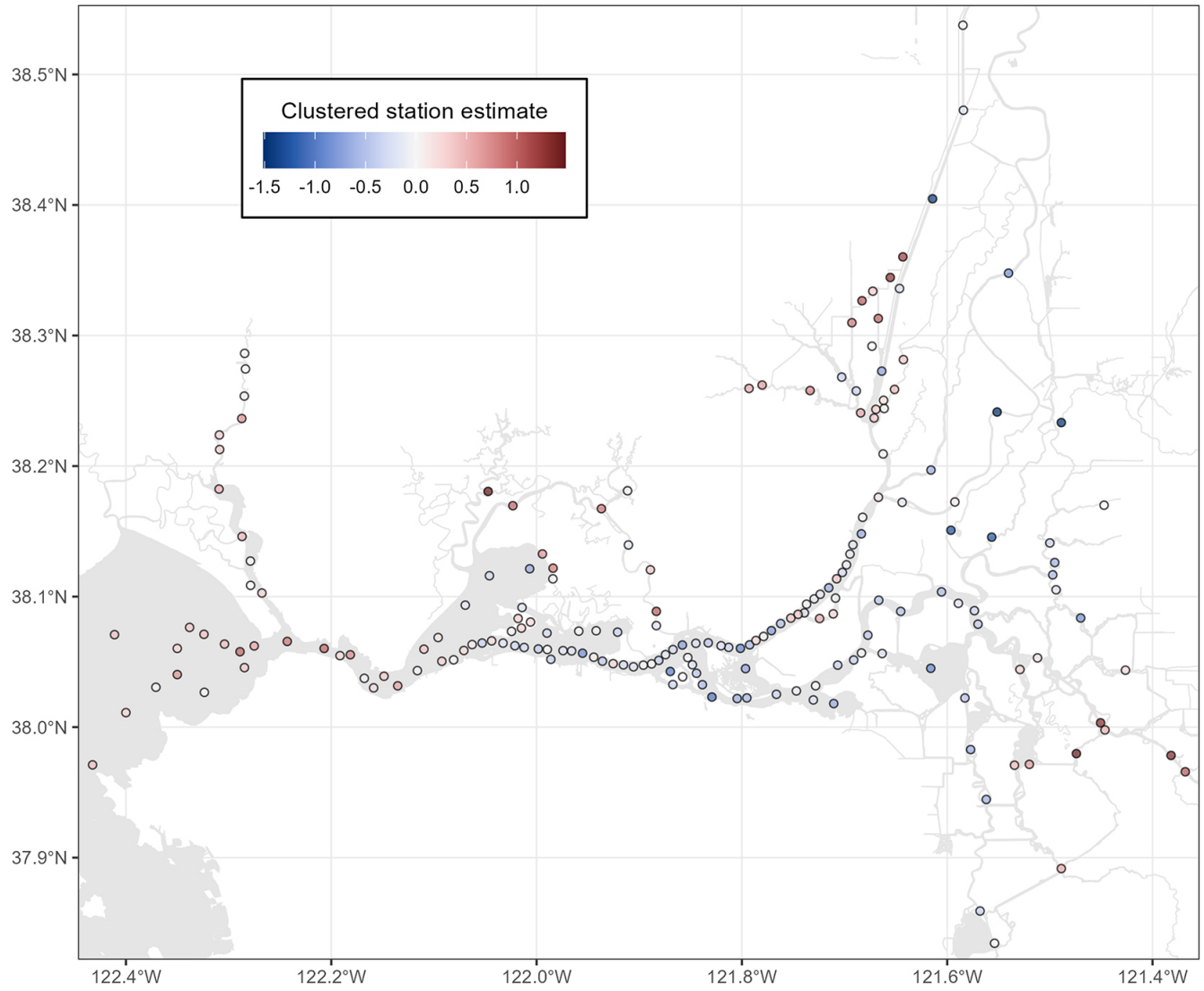

Figure 8 Estimated values of the station cluster random intercepts for *Acanthocyclops* spp. adults. See Figure 5 for a full description.

Seasonal Abundance Patterns

Currently, *B. longirostris* and *Acanthocyclops* spp. adults peak in the spring while *A. sinensis* adults peak in the fall and juveniles peak in the summer. The spring peaks line up with the spawning of Delta Smelt, while the summer and fall peaks provide critical food for Delta Smelt juveniles and young-of-the-year (Slater and Baxter 2014; Slater et al. 2019). The spring peaks also correspond to the out-migration of juvenile salmon and could provide food necessary to increase growth rates (Herbold et al. 2018; Phillis et al. 2018; Zeug et al. 2019) and reduce oceanic predation risks since larger fishes have lower predation risk (Sogard 1997).

Salinity Abundance Patterns

Bosmina longirostris and *Acanthocyclops* spp. are also both most abundant in the lowest-salinity bins (salinity < ~1), although *Acanthocyclops* spp. has a broader and higher salinity range potentially because of the different tolerances of the species in the complex. Freshwater habitat, especially in the spring, is where spawning for most native fish species occurs, including Delta Smelt and Sacramento Splittail (Moyle 2002). *Acartiella sinensis* peaks in more saline water

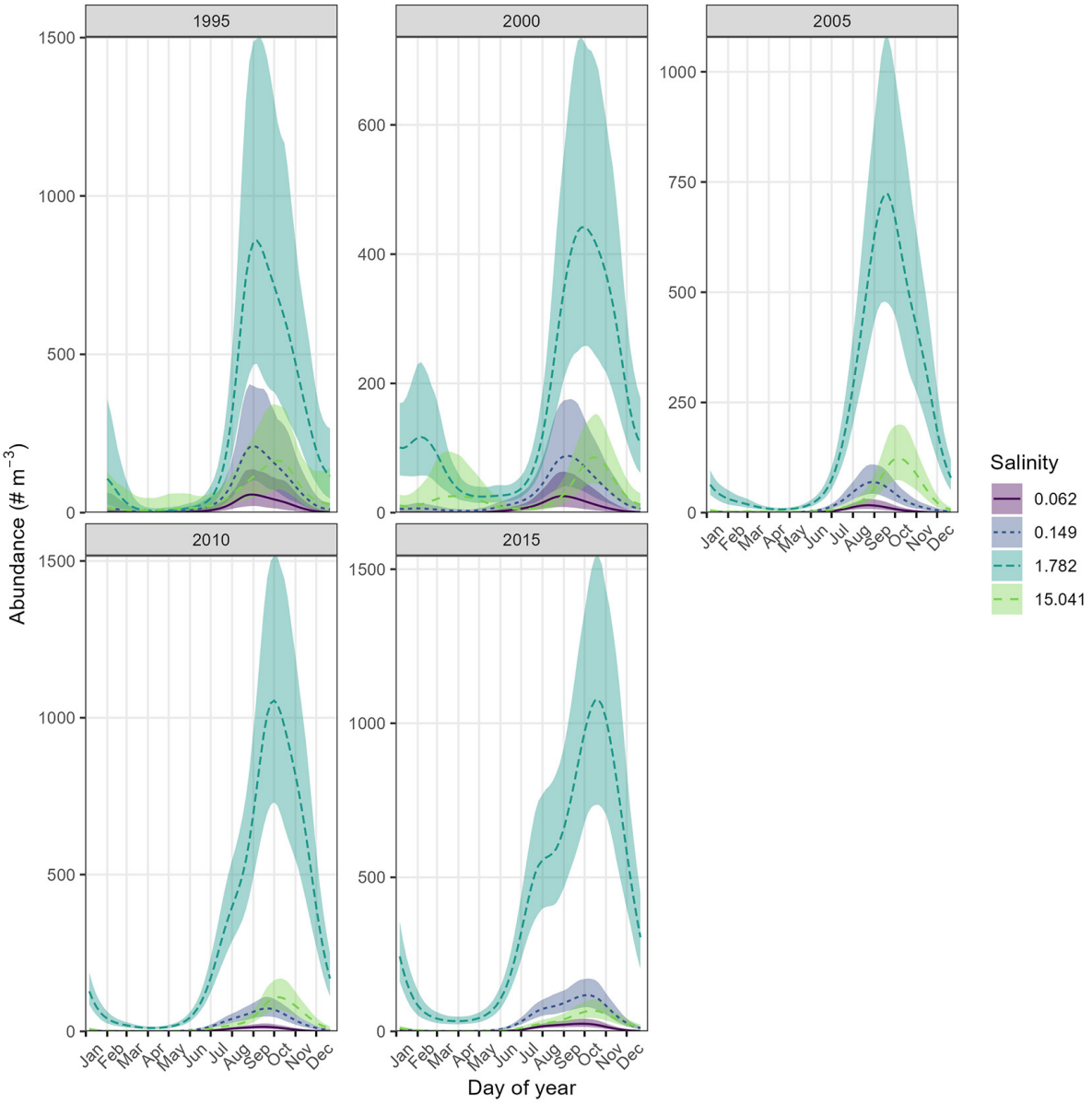

Figure 9 Seasonal patterns in *Acartiella sinensis* adult abundance with 99% credible intervals. See Figure 3 for a full description.

(~1 to 4) corresponding to the Low-Salinity Zone, which is a key habitat for rearing Delta Smelt (Sommer and Mejia 2013). Juvenile *A. sinensis* have a narrower salinity range and are abundant in more saline waters than the adults. The brackish and low-salinity habitats are important rearing habitats for many native fishes that evolved in highly variable conditions, giving native fishes an advantage over non-native fishes (Moyle et al. 2010), so an abundance of *Acanthocylops* spp. in brackish habitats may provide important food for rearing native fishes. Both *Acanthocyclops* spp. and *A. sinensis* are found in the diets of Longfin Smelt (Appendix A), which spawn and rear at slightly higher salinities than many other native fishes (Hobbs et al. 2006; Grimaldo et al. 2017; Jungbluth et al. 2021).

Interestingly, abundance peaks of juvenile *A. sinensis* were regularly 1 to 2 months later in the highest salinity bin (16.575) than in any of the lower salinities, which all peaked around

https://doi.org/10.15447/sfews.2023v21iss3art1

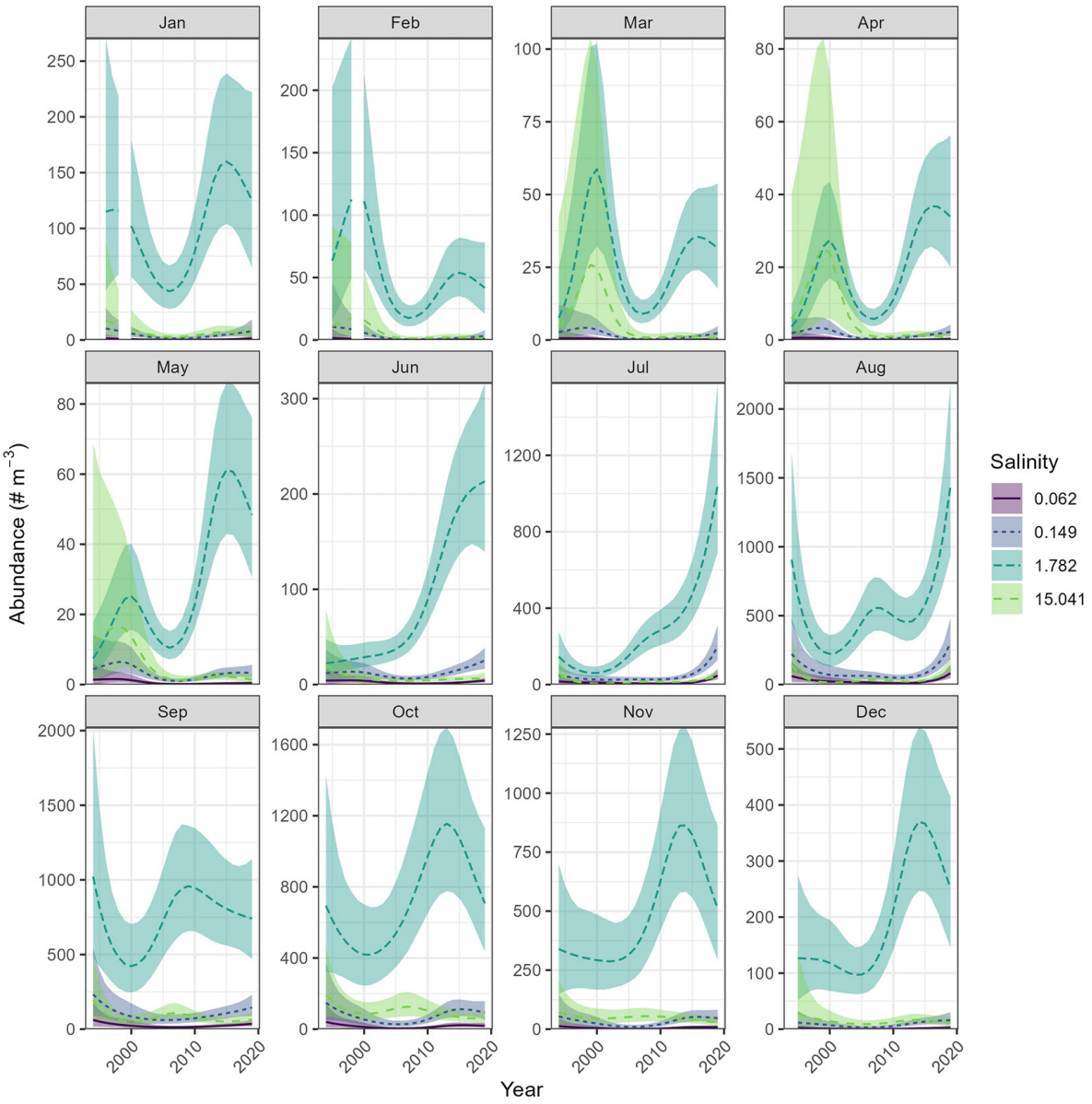

Figure 10 Yearly patterns in *Acartiella sinensis* adult abundance with 99% credible intervals. See Figure 4 for a full description.

the same time. This may reflect movement of *A. sinensis* (either juveniles or reproductive adults) into more saline waters from the late summer to fall. *Acartiella sinensis* exhibit tidal vertical migration behaviors (Kimmerer et al. 2002) that, depending on their interactions with tidal currents, could result in geographic movement or maintenance of a fixed geographic position. Geographic movement seaward could result in the observed pattern, as could maintenance of a fixed geographic position as salt intrudes further landward during the late summer to fall (Enright and Culberson 2009).

Geographic Abundance Patterns

Bosmina longirostris and *Acanthocyclops* spp. had similar geographic patterns, with their highest abundances (controlling for other covariates) in the Cache Slough Complex and the southeastern and eastern boundaries of the study region. *Bosmina longirostris* especially seemed to peak in areas of high residence time such as the

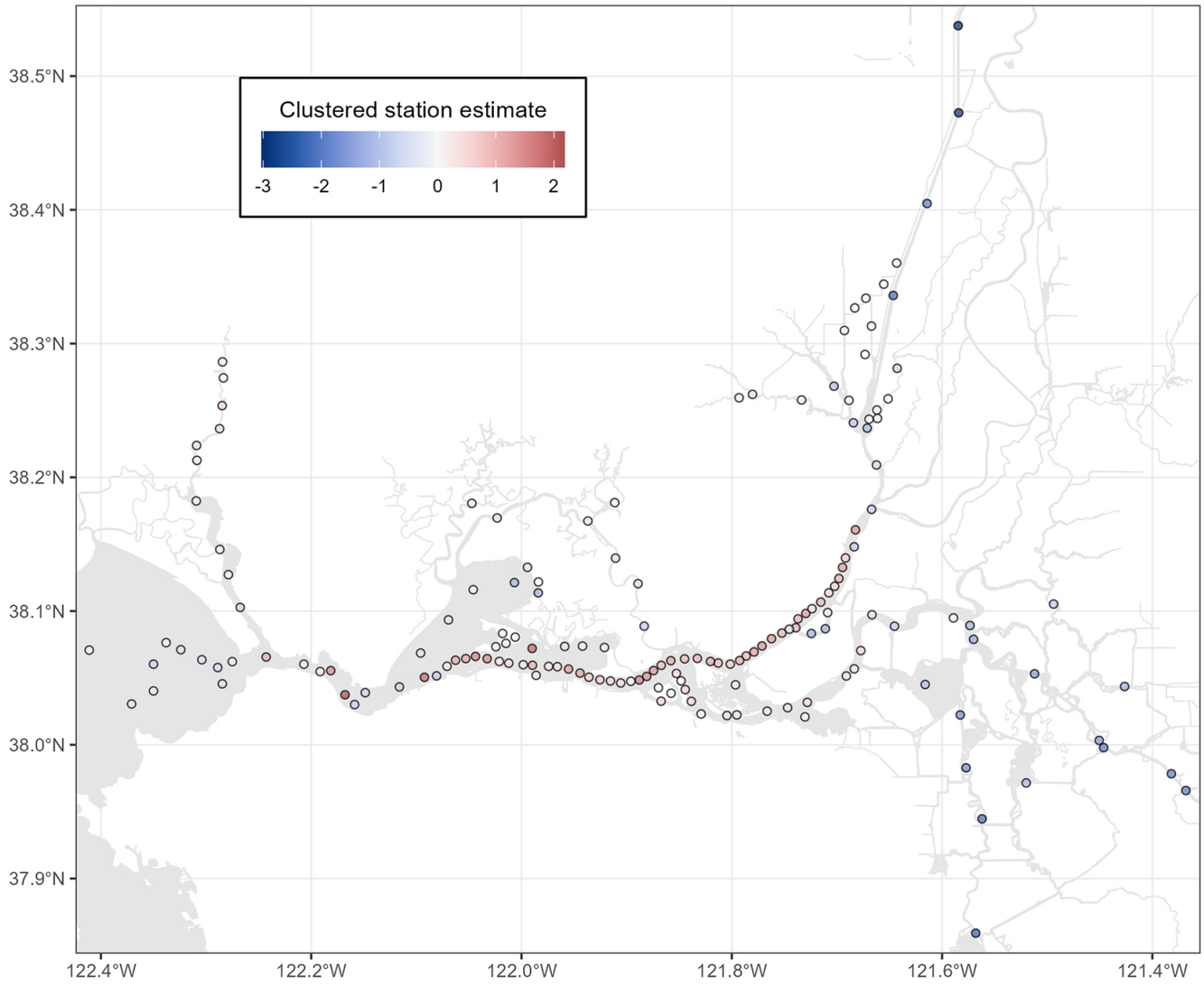

Figure 11 Estimated values of the station cluster random intercepts for *Acartiella sinensis* adults. See Figure 5 for a full description.

northernmost location on the Sacramento Deep Water Ship Channel and areas in the East Delta (Vroom et al. 2017; Lenoch et al. 2021). The Sacramento Deep Water Ship Channel is an important last refuge for Delta Smelt and other fishes (Young et al. 2021). *Acanthocyclops* spp. had very high geographic peaks in Suisun Marsh and Cache Slough, both areas with remnant and restored tidal wetlands that are important habitats for native fishes (Moyle et al. 2016; Colombano et al. 2020). *Bosmina longirostris* and *Acanthocyclops* spp. also had generally low abundance from Suisun Bay upstream (eastward) through the lower Sacramento and San Joaquin rivers, which was the region of highest abundance for *A. sinensis* adults.

Long-Term Changes

While *B. longirostris* and *Acanthocyclops* spp. have experienced overall declines in abundance over time, *A. sinensis* has mostly increased, although over a shorter time-period. The declines of *B. longirostris* and *Acanthocyclops* spp. correspond to noted regime shifts and overall plankton declines across many species (Winder and Jassby 2011). *Acartiella sinensis* was introduced at the end of this regime shift and was not subjected to the same declines.

https://doi.org/10.15447/sfews.2023v21iss3art1

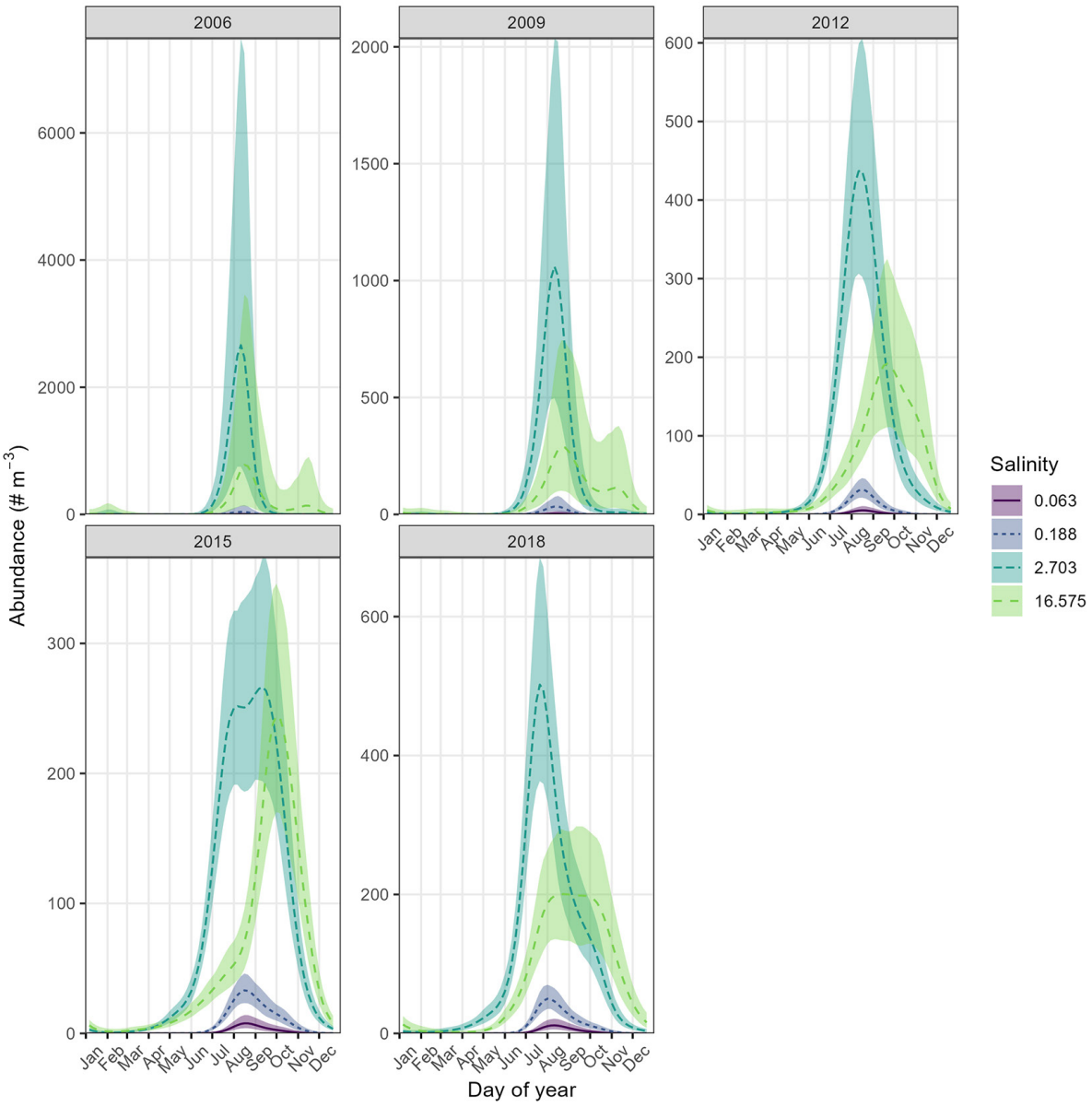

Figure 12 Seasonal patterns in *Acartiella sinensis* juvenile abundance with 99% credible intervals. See Figure 3 for a full description.

The change to the seasonal pattern of *B. longirostris* may have been the result of major environmental changes, including water operations and introduced species, but the precise mechanism is unclear. Before 1990, *B. longirostris* experienced two peaks, one in the spring and a second peak in the fall. In the late 1980s, *B. longirostris* abundance crashed during the fall. One potential explanation is changes to the operation of the State Water Project and Central Valley Project. Project operations cause a decrease in residence time in the South Delta (Hammock et al. 2019), which can reduce local phytoplankton abundance (Jassby et al. 2002; Hammock et al. 2019). However, project exports steadily increased from 1960 to 1980 before leveling off (Hammock et al. 2019), well before the disappearance of the fall peak of *B. longirostris*. Thus, the export explanation is unlikely to be the main factor driving the decrease.

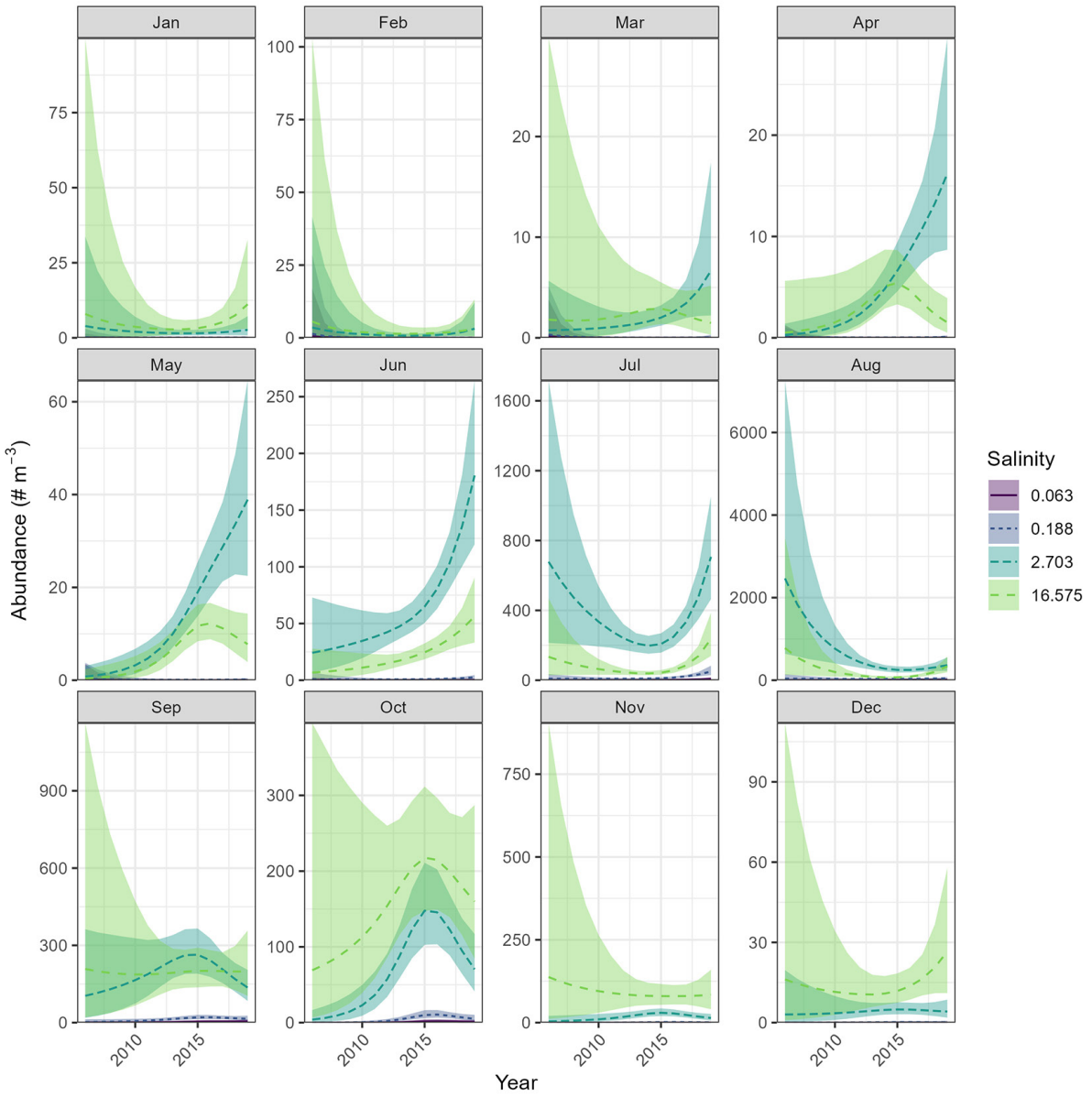

Figure 13 Yearly patterns in *Acartiella sinensis* juvenile abundance with 99% credible intervals. See Figure 4 for a full description.

Introduced species may be a more likely explanation for the change in the seasonal peaks of *B. longirostris*. The calanoid copepod *P. forbesi* was introduced in 1987 and quickly became the most abundant calanoid in the system (Orsi and Walter 1991). *Pseudodiaptomus forbesi* peaks in abundance from July through August, overlapping with the beginning of the historical peak in *B. longirostris* abundance, and they occur in high abundances in low salinities (Kayfetz and Kimmerer 2017), overlapping in salinity with *B. longirostris*. *Pseudodiaptomus forbesi* may be competing with *B. longirostris* for food resources during the fall during earlier years when most other zooplankton had peaked earlier in the year. *Bosmina longirostris* and *P. forbesi* both eat a wide range of phytoplankton, bacteria, and vascular plant detritus (DeMott and Kerfoot 1982; Acharya et al. 2005; Holmes and Kimmerer 2022), and while direct competition is difficult to directly observe, it is a possible explanation for the patterns we detected. Alternatively, the

https://doi.org/10.15447/sfews.2023v21iss3art1

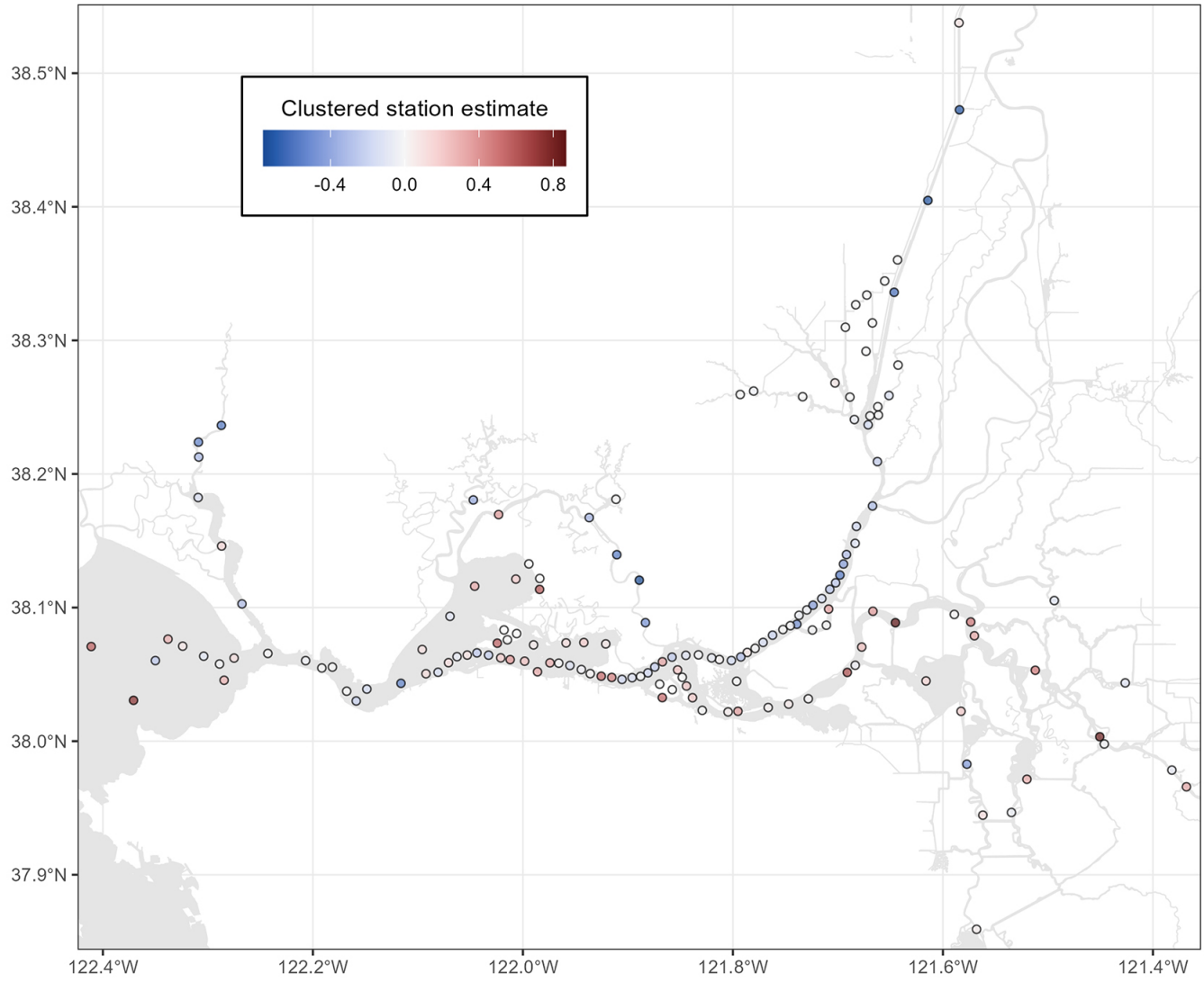

Figure 14 Estimated values of the station cluster random intercepts for *Acartiella sinensis* juveniles. See Figure 5 for a full description.

facilitation of a common predator would produce the same observed pattern.

The precipitous decline of *Acanthocyclops* spp. abundance may be related to the introduction of the cyclopoid *L. tetraspina* in 1993 (Orsi and Ohtsuka 1999). Before this introduction, *Acanthocyclops* spp. was the most abundant cyclopoid in the region (Orsi and Mecum 1986). After 1994, *L. tetraspina* quickly dominated the copepod community (Hennessy 2018) with *Acanthocyclops* spp. averaging ~1% of the abundance of *L. tetraspina* (Bashevkin et al. 2020). The introduction of *L. tetraspina* could have facilitated the decline of *Acanthocyclops* spp. through facilitation of a common predator, *A. sinensis*, as it likely did for *P. forbesi* (Kayfetz and Kimmerer 2017).

The strength of the relationship between *Acanthocyclops* spp. and salinity decreased over time. Before 2000, they were most abundant at salinities around 0.3, and after 2000 they were roughly equally abundant at a broad range of salinities from 0.6 to 3.4. This is likely the result of the differing salinity tolerances of the species within the complex, and changes in the relative abundances of those species over

time. Unfortunately, we do not have data on the abundances of each species in the complex so we cannot untangle the individual patterns. While *A. vernalis* has been described as native to the estuary (Orsi and Mecum 1986; Kratina and Winder 2015) in past literature, more recently the presence of the *A. vernalis* species complex has been confirmed in the estuary (Jungbluth et al 2021). Thus, it is unknown which species could be native, or if some were introduced during the study period. The strong relationship with salinity in early years (Figure B2) may indicate that one or more species with lower salinity tolerances initially dominated. Then, the diminishment of that relationship with salinity in later years may have been caused by the introduction and expansion of species with higher salinity tolerances within the complex, such as *A. americanus,* which has been found in high-salinity areas including the Mediterranean Sea (Alekseev 2021). The shift in phytoplankton communities caused by the introduction of *Potamocorbula amurensis* (Lucas et al. 2016), could also have contributed to this change by becoming the most important limiting abundance factor, rather than salinity. A reduction in food quantity or quality could have reduced the salinity abundance peak around 0.3, resulting in the flattening of the salinity–abundance relationship that we observed after 2000.

Abundance of *A. sinensis* became more strongly related to salinity over time. In the earlier years (before 2005), they were present in all salinities in our study, and even equally abundant in high salinities of 15 and low salinities of 0.15. They also exhibited a unique winter–spring abundance peak in the two highest salinities that disappeared by 2005. Because they were first detected in the estuary in 1993 (Orsi and Ohtsuka 1999), this pattern could reflect them settling into their ecological niche over time, or alterations to predation or food supply from the Pelagic Organism Decline regime change.

Interestingly, *A. sinensis* juveniles had increasingly wide seasonal abundance peaks over time, driven in part by differing timing of abundance peaks in the two highest-salinity bins. As noted above (Salinity Abundance Patterns), abundance peaks were regularly 1 to 2 months later in the highest-salinity bin (16.575) than in the lower salinities. The abundance peak in the highest-salinity bin also grew larger than that of the lower salinities over the years, which led to an overall widening of the seasonal abundance peak for *A. sinensis* juveniles. However, the width of the abundance peak in each lower-salinity bin also seemed to increase over time. This demonstrates the shifting phenology of *A. sinensis,* which could be caused by changes in the timing and location of reproduction, predation, or feeding. The zooplankton community has undergone many shifts over the history of this data set (Orsi and Ohtsuka 1999; Winder and Jassby 2011), with *A. sinensis* potentially having its own effects on lower-trophic-level zooplankton (Kayfetz and Kimmerer 2017). Since *A. sinensis* is predatory, its abundance peaks could be following (in salinity, space, and time) the abundance shifts of other species, resulting in changes to the location and timing of its reproduction, and thus affecting the abundance of both adult and juvenile *A. sinensis*.

CONCLUSIONS

Many of the fishes in the estuary rely on zooplankton for at least part of their life cycle (Appendix A). Changes in prey resources can affect higher trophic levels by reducing the amount of available food or shifting the timing of peak abundance, thereby creating a mismatch between critical fish life stages and their prey. We found long-term shifts in all three of our study taxa. These shifts included changes in seasonality, relationships to salinity, and long-term abundance. Further studies that investigate these patterns in additional species would be important to understand the past dynamics of zooplankton in the estuary. These results increase our understanding of the zooplankton community, which could inform the development of food-web models and be matched to trends in fish abundance to examine how declining zooplankton species directly affect managed species.

https://doi.org/10.15447/sfews.2023v21iss3art1

ACKNOWLEDGMENTS

This work was conducted under the auspices of the Interagency Ecological Program (IEP). Funding for the IEP work plan element (062) CDFW Quantitative Analysis of Stomach Contents and Body Weight for Pelagic Fishes ("Diet and Condition Study") that collected the diet data was provided by contracts with the Department of Water Resources (R1730002) and the US Bureau of Reclamation (R20AC00089). The authors would like to thank Laurel Larsen, Steve Slater, Wim Kimmerer, David Senn, and an anonymous reviewer for comments on this manuscript, and the field and laboratory staff of the Stockton CDFW office—particularly Tricia Bippus, Phillip Poirier, and Tom Gabel—for their tireless work in collecting and processing zooplankton and fish diet samples. Lastly, the authors would like to thank Tricia Bippus, Anne Slaughter, and Michelle Avila for the zooplankton photos in Figure 1.

REFERENCES

Acharya K, Jack JD, Bukaveckas PA. 2005. Dietary effects on life history traits of riverine Bosmina. Freshw Biol. [accessed 2023 Sep 20];50(6):965–975. *https://doi.org/10.1111/j.1365-2427.2005.01379.x*

Adamczuk M. 2016. Past, present, and future roles of small cladoceran *Bosmina longirostris* (O. F. Müller, 1785) in aquatic ecosystems. Hydrobiologia. [accessed 2023 Sep 20];767(1):1–11. *https://doi.org/10.1007/s10750-015-2495-7*

Adamczuk M, Mieczan T. 2019. Within-species phenotypic diversity enhances resistance to stress - a case study using the polymorphic species *Bosmina longirostris*. Intl Rev Hydrobiology. [accessed 2023 Sep 20];104(5–6):137–146. *https://doi.org/10.1002/iroh.201901985*

Alekseev V, Fefilova E, Dumont H. 2002. Some noteworthy free-living copepods from surface freshwater in Belgium. Belgian J Zool. [accessed 2023 Sep 20];132(2):133–139. *https://biblio.ugent.be/publication/363636/file/457939*

Alekseev VR. 2021. Confusing invader: *Acanthocyclops americanus* (Copepoda: Cyclopoida) and its biological, anthropogenic and climate-dependent mechanisms of rapid distribution in Eurasia. Water. [accessed 2023 Sep 20];13(10):1423. *https://doi.org/10.3390/w13101423*

Ambler JW, Cloern JE, Hutchinson A. 1985. Seasonal cycles of zooplankton from San Francisco Bay. In: Cloern JE, Nichols FH, editors. Temporal dynamics of an estuary: San Francisco Bay. Dordrecht (Netherlands): Springer. (Developments in Hydrobiology). [accessed 2020 May 18]. p. 177–197. *https://doi.org/10.1007/978-94-009-5528-8_11*

Anderson RS. 1970. Predator–prey relationships and predation rates for crustacean zooplankters from some lakes in western Canada. Can J Zool. [accessed 2023 Sep 20];48(6):1229–1240. *https://doi.org/10.1139/z70-212*

Balcer MD, Korda NL, Dodson SI. 1984. Zooplankton of the Great Lakes: a guide to the identification and ecology of the common crustacean species. Madison (WI): University of Wisconsin Press. [accessed 2023 Sep 20]. 188 p.

Barros A, Hobbs JA, Willmes M, Parker CM, Bisson M, Fangue NA, Rypel AL, Lewis LS. 2022. Spatial heterogeneity in prey availability, feeding success, and dietary selectivity for the threatened Longfin Smelt. Estuar Coasts. [accessed 2022 Jan 12];45:1766-1779. *https://doi.org/10.1007/s12237-021-01024-y*

Bashevkin SM. 2021. zooper: an R package to download and integrate zooplankton datasets from the upper San Francisco Estuary. Version 2.2.0. Zenodo. [accessed 2021 Jun 10]. *https://doi.org/10.5281/zenodo.4923868*

Bashevkin SM, Hartman R, Thomas M, Barros A, Burdi C, Hennessy A, Tempel T, Kayfetz K. 2020. Interagency Ecological Program: zooplankton abundance in the upper San Francisco Estuary from 1972-2018, an integration of 5 long-term monitoring programs. Environmental Data Initiative. [accessed 2020 Jun 10]. *https://doi.org/10.6073/PASTA/0C400C670830E4C8F7FD45C187EFDCB9*

Bashevkin SM, Hartman R, Thomas M, Barros A, Burdi CE, Hennessy A, Tempel T, Kayfetz K. 2022. Five decades (1972–2020) of zooplankton monitoring in the upper San Francisco Estuary. PLoS ONE. [accessed 2023 Sep 20];17(3):e0265402. *https://doi.org/10.1371/journal.pone.0265402*

Bouley P, Kimmerer WJ. 2006. Ecology of a highly abundant, introduced cyclopoid copepod in a temperate estuary. Mar Ecol Prog Ser. [accessed 2023 Sep 20];324:219–228. *https://doi.org/10.3354/meps324219*

Brown LR, Bauer ML. 2010. Effects of hydrologic infrastructure on flow regimes of California's Central Valley rivers: implications for fish populations. River Res Appl. [accessed 2023 Sep 20];26(6):751–765. *https://doi.org/10.1002/rra.1293*

Brown LR, Kimmerer W, Conrad JL, Lesmeister S, Mueller–Solger A. 2016. Food webs of the Delta, Suisun Bay, and Suisun Marsh: an update on current understanding and possibilities for management. San Franc Estuary Watershed Sci. [accessed 2019 Aug 6];14(3). *http://doi.org/10.15447/sfews.2016v14iss3art4*

Bürkner P-C. 2017. brms: an R package for Bayesian multilevel models using Stan. J Stat Softw. [accessed 2023 Sep 20];80(1):1–28. *https://doi.org/10.18637/jss.v080.i01*

Bürkner P-C. 2018. Advanced Bayesian multilevel modeling with the R package brms. The R Journal. [accessed 2023 Sep 20];10(1):395–411. *https://doi.org/10.32614/RJ-2018-017*

Carpenter SR, Kitchell JF. 1984. Plankton community structure and limnetic primary production. Am Nat. [accessed 2023 Sep 20];124(2):159–172. *https://doi.org/10.1086/284261*

Chigbu P, Sibley TH. 1998a. Predation by Longfin Smelt (*Spirinchus thaleichthys*) on the mysid *Neomysis mercedis* in Lake Washington. Freshw Biol. [accessed 2023 Sep 20];40(2):295–304. *https://doi.org/10.1046/j.1365-2427.1998.00354.x*

Chigbu P, Sibley TH. 1998b. Feeding ecology of Longfin Smelt (*Spirinchus thaleichthys* Ayres) in Lake Washington. Fish Res. [accessed 2023 Sep 20];38(2):109–119. *https://doi.org/10.1016/S0165-7836(98)00156-8*

Colombano DD, Manfree AD, O'Rear TA, Durand JR, Moyle PB. 2020. Estuarine-terrestrial habitat gradients enhance nursery function for resident and transient fishes in the San Francisco Estuary. Mar Ecol Prog Ser. [accessed 2023 Sep 20];637:141–157. *https://doi.org/10.3354/meps13238*

Corline NJ, Peek RA, Montgomery J, Katz JVE, Jeffres CA. 2021. Understanding community assembly rules in managed floodplain food webs. Ecosphere. [accessed 2023 Sep 20];12(2):e03330. *https://doi.org/10.1002/ecs2.3330*

Craddock DR, Blahm TH, Parente WD. 1976. Occurrence and utilization of zooplankton by juvenile Chinook Salmon in the lower Columbia River. Trans Am Fish Soc. [accessed 2023 Sep 20];105(1):72–76. *https://doi.org/10.1577/1548-8659(1976)105<72:OAUOZB>2.0.CO;2*

Cushing DH. 1969. The regularity of the spawning season of some fishes. ICES J Mar Sci. [accessed 2023 Sep 20];33(1):81–92. *https://doi.org/10.1093/icesjms/33.1.81*

Cushing DH. 1990. Plankton production and year-class strength in fish populations: an update of the match/mismatch hypothesis. In: Blaxter JHS, Southward AJ, editors. Advances in marine biology. Vol. 26. Cambridge (MA): Academic Press Inc. (Elsevier). p. 249–293. [accessed 2020 Jul 6]. Available from: *http://www.sciencedirect.com/science/article/pii/S0065288108602023*

DeMott WR, Kerfoot WC. 1982. Competition among cladocerans: nature of the interaction between *Bosmina* and *Daphnia*. Ecology. [accessed 2023 Sep 20];63(6):1949–1966. *https://doi.org/10.2307/1940132*

Dodson SI, Grishanin Andrey K, Gross K, Wyngaard GA. 2003. Morphological analysis of some cryptic species in the *Acanthocyclops vernalis* species complex from North America. Hydrobiologia. [accessed 2023 Sep 20];500(1):131–143. *https://doi.org/10.1023/A:1024678018090*

Drenner RW, Vinyard GL, O'Brien WJ, Triplett JR, Wagner J. 1981. The zooplankton community of Lacygne Lake: a cooling pond in Kansas. Southwestern Nat. [accessed 2023 Sep 20];26(3):243–249. *https://doi.org/10.2307/3670904*

Durant JM, Hjermann DØ, Ottersen G, Stenseth NC. 2007. Climate and the match or mismatch between predator requirements and resource availability. Clim Res. [accessed 2023 Sep 20];33(3):271–283. *https://doi.org/10.3354/cr033271*

Edwards M, Richardson AJ. 2004. Impact of climate change on marine pelagic phenology and trophic mismatch. Nature. [accessed 2023 Sep 20];430(7002):881–884. *https://doi.org/10.1038/nature02808*

Enright C, Culberson SD. 2009. Salinity trends, variability, and control in the northern reach of the San Francisco Estuary. San Franc Estuary Watershed Sci. [accessed 2021 Nov 12];7(2). *https://doi.org/10.15447/sfews.2009v7iss2art3*

Enríquez-García C, Nandini S, Sarma SSS. 2013. Feeding behaviour of *Acanthocyclops americanus* (Marsh) (Copepoda: Cyclopoida). J Nat Hist. [accessed 2023 Sep 20];47(5–12):853–862. *https://doi.org/10.1080/00222933.2012.747637*

Evans MS, Stewart JA. 1977. Epibenthic and benthic microcrustaceans (copepods, cladocerans, ostracods) from a nearshore area in southeastern Lake Michigan1. Limnol Oceanogr. [accessed 2023 Sep 20];22(6):1059–1066. *https://doi.org/10.4319/lo.1977.22.6.1059*

Feyrer F, Nobriga ML, Sommer TR. 2007. Multidecadal trends for three declining fish species: habitat patterns and mechanisms in the San Francisco Estuary, California, USA. Can J Fish Aquat Sci. [accessed 2023 Sep 20];64(4):723–734. *https://doi.org/10.1139/f07-048*

Gliwicz ZM, Stibor H. 1993. Egg predation by copepods in *Daphnia* brood cavities. Oecologia. [accessed 2023 Sep 20];95(2):295–298. *https://doi.org/10.1007/BF00323503*

Goertler P, Jones K, Cordell J, Schreier B, Sommer T. 2018. Effects of extreme hydrologic regimes on juvenile Chinook Salmon prey resources and diet composition in a large river floodplain. Trans Am Fish Soc. [accessed 2023 Sep 20];147(2):287–299. *https://doi.org/10.1002/tafs.10028*

Gräler B, Pebesma E, Heuvelink G. 2016. Spatio-temporal interpolation using gstat. RFID J. [accessed 2023 Sep 20];8(1):204–218.

Grimaldo L, Feyrer F, Burns J, Maniscalco D. 2017. Sampling uncharted waters: examining rearing habitat of larval Longfin Smelt (*Spirinchus thaleichthys*) in the upper San Francisco Estuary. Estuaries Coasts. [accessed 2023 Sep 20];40(6):1771–1784. *https://doi.org/10.1007/s12237-017-0255-9*

Hammock BG, Moose SP, Solis SS, Goharian E, Teh SJ. 2019. Hydrodynamic modeling coupled with long-term field data provide evidence for suppression of phytoplankton by invasive clams and freshwater exports in the San Francisco Estuary. Environ Manag. [accessed 2023 Sep 20];63(6):703–717. *https://doi.org/10.1007/s00267-019-01159-6*

Hart RC. 2004. Cladoceran Periodicity patterns in relation to selected environmental factors in two cascading warm-water reservoirs over a decade. Hydrobiologia. [accessed 2023 Sep 20];526(1):99–117. *https://doi.org/10.1023/B:HYDR.0000041610.56021.63*

Hennessy A. 2018. Zooplankton monitoring 2017. Interagency Ecological Program Newsletter. [accessed 2023 Sep 20];32(1):21–32.

Herbold B, Carlson SM, Henery R, Johnson RC, Mantua N, McClure M, Moyle PB, Sommer T. 2018. Managing for salmon resilience in California's variable and changing climate. San Franc Estuary Watershed Sci. [accessed 2022 Jan 12];16(2). *https://doi.org/10.15447/sfews.2018v16iss2art3*

Hobbs JA, Bennett WA, Burton JE. 2006. Assessing nursery habitat quality for native smelts (Osmeridae) in the low-salinity zone of the San Francisco Estuary. J Fish Biol. [accessed 2023 Sep 20];69(3):907–922. *https://doi.org/10.1111/j.1095-8649.2006.01176.x*

Holm J-Chr, Møller D. 1984. Growth and prey selection by Atlantic salmon yearlings reared on live freshwater zooplankton. Aquaculture. [accessed 2023 Sep 20];43(4):401–412. *https://doi.org/10.1016/0044-8486(84)90248-5*

Holmes AE, Kimmerer WJ. 2022. Phytoplankton prey of an abundant estuarine copepod identified in situ using DNA metabarcoding. J Plank Res. [accessed 2023 Sep 20];44(2):316–332. *https://doi.org/10.1093/plankt/fbac002*

Hunter JR. 1981. Feeding ecology and predation of marine fish larvae. In: Lasker R, editor. Marine fish larvae: morphology, ecology, and relation to fisheries. Vol. 1. Seattle (WA): University of Washington Press. p. 33–77.

Hutton PH, Rath JS, Roy SB. 2017. Freshwater flow to the San Francisco Bay-Delta estuary over nine decades (part 1): trend evaluation. Hydrol Process. [accessed 2023 Sep 20];31(14):2500–2515. https://doi.org/10.1002/hyp.11201

Inpang R. 2008. Annual changes of zooplankton communities of different size fractions in Thale-Noi, Phatthalung Province [M.Sc Thesis]. [Hat Yai (Thailand)]: Prince of Songkla University.

Jassby AD, Cloern JE, Cole BE. 2002. Annual primary production: patterns and mechanisms of change in a nutrient-rich tidal ecosystem. Limnol Oceanogr. [accessed 2023 Sep 20];47(3):698–712. https://doi.org/10.4319/lo.2002.47.3.0698

Jeffres CA, Holmes EJ, Sommer TR, Katz JVE. 2020. Detrital food web contributes to aquatic ecosystem productivity and rapid salmon growth in a managed floodplain. PLoS ONE. [accessed 2023 Sep 20];15(9):e0216019. https://doi.org/10.1371/journal.pone.0216019

Jiang X, Li Q, Liang H, Zhao S, Zhang L, Zhao Y, Chen L, Yang W, Xiang X. 2013. Clonal variation in growth plasticity within a *Bosmina longirostris* population: the potential for resistance to toxic cyanobacteria. PLoS ONE. [accessed 2023 Sep 20];8(9):e73540. https://doi.org/10.1371/journal.pone.0073540

Jiang X, Xie J, Xu Y, Zhong W, Zhu X, Zhu C. 2017. Increasing dominance of small zooplankton with toxic cyanobacteria. Freshw Biol. [accessed 2023 Sep 20];62(2):429–443. https://doi.org/10.1111/fwb.12877

Jiang X, Yang W, Xiang X, Niu Y, Chen L, Zhang J. 2014. Cyanobacteria alter competitive outcomes between *Daphnia* and *Bosmina* in dependence on environmental conditions. Fund Appl Limnol. [accessed 2023 Sep 20];184(1):11–22. [DOI?]

Jungbluth MJ, Burns J, Grimaldo L, Slaughter A, Katla A, Kimmerer W. 2021. Feeding habits and novel prey of larval fishes in the northern San Francisco Estuary. Environmental DNA. [accessed 2023 Sep 20];3(6):1059–1080. https://doi.org/10.1002/edn3.226

Jürgens K, Wickham SA, Rothhaupt KO, Santer B. 1996. Feeding rates of macro- and microzooplankton on heterotrophic nanoflagellates. Limnol Oceanogr. [accessed 2023 Sep 20];41(8):1833–1839. https://doi.org/10.4319/lo.1996.41.8.1833

Kayfetz K, Bashevkin SM, Thomas M, Hartman R, Burdi CE, Hennessy A, Tempel T, Barros A. 2020. Zooplankton integrated dataset metadata report. IEP Technical Report. 93. Sacramento (CA): California Department of Water Resources. 45 p.

Kayfetz K, Kimmerer W. 2017. Abiotic and biotic controls on the copepod *Pseudodiaptomus forbesi* in the upper San Francisco Estuary. Mar Ecol Prog Ser. [accessed 2023 Sep 20];581:85–101. https://doi.org/10.3354/meps12294

Kerfoot WC. 1978. Combat between predatory copepods and their prey: *Cyclops, Epischura,* and *Bosmina*. Limnol Oceanogr. [accessed 2023 Sep 20];23(6):1089–1102. https://doi.org/10.4319/lo.1978.23.6.1089

Kimmerer W. 2004. Open water processes of the San Francisco Estuary: from physical forcing to biological responses. San Franc Estuary Watershed Sci. [accessed 2020 Mar 24]. 2(1). https://doi.org/10.15447/sfews.2004v2iss1art1

Kimmerer W, Ignoffo TR, Bemowski B, Modéran J, Holmes A, Bergamaschi B. 2018. Zooplankton dynamics in the Cache Slough complex of the upper San Francisco Estuary. San Franc Estuary Watershed Sci. [accessed 2020 May 21];16(3). https://doi.org/10.15447/sfews.2018v16iss3art4

Kimmerer WJ. 2002. Physical, biological, and management responses to variable freshwater flow into the San Francisco Estuary. Estuaries. [accessed 2023 Sep 20];25(6):1275–1290. https://doi.org/10.1007/BF02692224

Kimmerer WJ, Burau JR, Bennett WA. 2002. Persistence of tidally-oriented vertical migration by zooplankton in a temperate estuary. Estuaries. [accessed 2023 Sep 20];25(3):359–371. https://doi.org/10.1007/BF02695979

Kimmerer WJ, Ignoffo TR, Slaughter AM, Gould AL. 2014. Food-limited reproduction and growth of three copepod species in the low-salinity zone of the San Francisco Estuary. J Plank Res. [accessed 2023 Sep 20];36(3):722–735. https://doi.org/10.1093/plankt/fbt128

Kratina P, Nally RM, Kimmerer WJ, Thomson JR, Winder M. 2014. Human-induced biotic invasions and changes in plankton interaction networks. J Appl Ecol. [accessed 2023 Sep 20];51(4):1066–1074. *https://doi.org/10.1111/1365-2664.12266*

Kratina P, Winder M. 2015. Biotic invasions can alter nutritional composition of zooplankton communities. Oikos. [accessed 2023 Sep 20];124(10):1337–1345. *https://doi.org/10.1111/oik.02240*

Lenoch LK, Stumpner PR, Burau JR, Loken LC, Sadro S. 2021. Dispersion and stratification dynamics in the upper Sacramento River Deep Water Ship Channel. San Franc Estuar Watershed Sci. [accessed 2021 Dec 16];19(4). *https://doi.org/10.15447/sfews.2021v19iss4art5.*

Lojkovic Burris ZP, Baxter RD, Burdi CE. 2022. Larval and juvenile Longfin Smelt diets as a function of fish size and prey density in the San Francisco Estuary. California Fish Wildl J. [accessed 2022 Jul 1];108(2). *https://doi.org/10.51492/cfwj.108.11*

Lucas LV, Cloern JE, Thompson JK, Stacey MT, Koseff JR. 2016. Bivalve grazing can shape phytoplankton communities. Front Mar Sci. [accessed 2023 Sep 20];3:14. *https://doi.org/10.3389/fmars.2016.00014*

Matveev VF, Balseiro EG. 1990. Contrasting responses of two cladocerans to changes in the nutritional value of nannoplankton. Freshw Biol. [accessed 2023 Sep 20];23(2):197–204.

McElreath R. 2015. Statistical rethinking: a Bayesian course with examples in R and Stan. Boca Raton (FL): CRC Press. 487 p.

Merz JE, Bergman PS, Simonis JL, Delaney D, Pierson J, Anders P. 2016. Long-term seasonal trends in the prey community of Delta Smelt (*Hypomesus transpacificus*) within the Sacramento-San Joaquin Delta, California. Estuar Coasts. [accessed 2023 Sep 20];39(5):1526–1536. *https://doi.org/10.1007/s12237-016-0097-x*

Miracle MR, Alekseev V, Monchenko V, Sentandreu V, Vicente E. 2013. Molecular-genetic-based contribution to the taxonomy of the *Acanthocyclops robustus* group. J Nat Hist. [accessed 2023 Sep 20];47(5–12):863–888. *https://doi.org/10.1080/00222933.2012.744432*

Moyle PB. 2002. Inland fishes of California: revised and expanded. [accessed 2023 Sep 20]. Berkeley (CA): University of California Press. 412 p. Available from: *https://www.ucpress.edu/book/9780520227545/inland-fishes-of-california*

Moyle PB, Brown LR, Durand JR, Hobbs JA. 2016. Delta Smelt: life history and decline of a once-abundant species in the San Francisco Estuary. San Franc Estuary Watershed Sci. [accessed 2019 Aug 6];14(2). *https://doi.org/10.15447/sfews.2016v14iss2art6.*

Moyle PB, Lund JR, Bennett WA, Fleenor WE. 2010. Habitat variability and complexity in the upper San Francisco Estuary. San Franc Estuary Watershed Sci. [accessed 2021 Feb 2];8(3). *https://doi.org/10.15447/sfews.2010v8iss3art1*

Onandia G, Dias JD, Miracle MR. 2015. Zooplankton grazing on natural algae and bacteria under hypertrophic conditions. Limnetica. [accessed 2023 Sep 20];34(2):541–560.

Orsi JJ, Mecum WL. 1986. Zooplankton distribution and abundance in the Sacramento-San Joaquin Delta in relation to certain environmental factors. Estuaries. [accessed 2023 Sep 20];9(4):326–339. *https://doi.org/10.2307/1351412*

Orsi JJ, Ohtsuka S. 1999. Introduction of the Asian copepods *Acartiella sinensis*, *Tortanus dextrilobatus* (Copepoda: Calanoida), and *Limnoithona tetraspina* (Copepoda: Cyclopoida) to the San Francisco Estuary, California, USA. Plank Biol Ecol. [accessed 2023 Sep 20];46(2):128–131. [DOI?].

Orsi JJ, Walter TE. 1991. *Pseudodiaptomus forbesi* and *P. marinus* (Copepoda Calanoida), the latest copepod immigrants to California's Sacramento-San Joaquin Estuary. In: Uye SI, Nishida S, Ho J-S, editors. Proc. Fourth Internl. Conf. on Copepoda. Hiroshima: Bull. Plankton Soc. Jpn. p. 553–562.

Pebesma EJ. 2004. Multivariable geostatistics in S: the gstat package. Comput Geosci. [accessed 2023 Sep 20];30(7):683–691. *https://doi.org/10.1016/j.cageo.2004.03.012*

Phillis CC, Sturrock AM, Johnson RC, Weber PK. 2018. Endangered winter-run Chinook Salmon rely on diverse rearing habitats in a highly altered landscape. Biol Conserv. [accessed 2023 Sep 20];217:358–362. *https://doi.org/10.1016/j.biocon.2017.10.023*

Piasecki WG. 2000. Attacks of cyclopoid *Acanthocyclops robustus* [Sars] on newly hatched cyprinids. Electr J Polish Agric Universities Series Fisheries. 1(03). [accessed 2021 Sep 3]. Available from: *https://www.infona.pl//resource/bwmeta1.element.agro-article-c69d1cf5-d408-436f-9b5e-810f38f00c59*

Roegner C, Bottom D, Baptista A, Campbell L, Goertler P, Hinton S, McNatt R, Simenstad C, Teel D, Fresh K. 2015. Salmon habitat use of tidal-fluvial habitats of the Columbia River Estuary, 2010-2013. Final report. Report of research by NOAA Fisheries, Northwest Fisheries Science Center to US Army Corps of Engineers, Portland District. 103 p.

Romare P. 2000. Growth of larval and juvenile perch: the importance of diet and fish density. J Fish Biol. [accessed 2023 Sep 20];56(4):876–889. *https://doi.org/10.1111/j.1095-8649.2000.tb00878.x*

Sarma SSS, Miracle MR, Nandini S, Vicente E. 2019. Predation by *Acanthocyclops americanus* (Copepoda: Cyclopoida) in the hypertrophic shallow waterbody, Lake Albufera (Spain): field and laboratory observations. Hydrobiologia. [accessed 2023 Sep 20];829(1):5–17. *https://doi.org/10.1007/s10750-018-3546-7*

Shen C-J, Lee F. 1963. The estuarine copepoda of Chiekong and Zaikong rivers, Kwangtung Province China. Acta Zool Sin. [accessed 2023 Sep 20];15:571–596.

Slater SB, Baxter RD. 2014. Diet, prey selection, and body condition of age-0 Delta Smelt, *Hypomesus transpacificus*, in the upper San Francisco Estuary. San Franc Estuary Watershed Sci. [accessed 2020 Jan 24];12(3). *http://doi.org/10.15447/sfews.2014v12iss3art1*

Slater SB, Schultz A, Hammock BG, Hennessy A, Burdi C. 2019. Patterns of zooplankton consumption by juvenile and adult Delta Smelt (*Hypomesus transpacifus*). In: Schultz A, editor. Directed Outflow Project Technical Report 1. [accessed 2023 Sep 20]. Sacramento (CA): US Bureau of Reclamation, Bay-Delta Office, Mid-Pacific Region. Available from: *https://www.usbr.gov/mp/bdo/docs/directed-outflow-project-tech-report1.pdf*

Slaughter AM, Ignoffo TR, Kimmerer W. 2016. Predation impact of *Acartiella sinensis*, an introduced predatory copepod in the San Francisco Estuary, USA. Mar Ecol Prog Ser. [accessed 2023 Sep 20];547:47–60. *https://doi.org/10.3354/meps11640*

Sogard SM. 1997. Size-selective mortality in the juvenile stage of teleost fishes: a review. Bull Mar Sci. [accessed 2023 Sep 20];60(3):1129–1157. *https://www.ingentaconnect.com/content/umrsmas/bullmar/1997/00000060/00000003/art00029*

Sommer T, Mejia F. 2013. A place to call home: a synthesis of Delta Smelt habitat in the upper San Francisco Estuary. San Franc Estuary Watershed Sci. [accessed 2021 May 13];11(2). *https://doi.org/10.15447/sfews.2013v11iss2art4*

Sommer TR, Armor C, Baxter R, Breuer R, Brown L, Chotkowski M, Culberson S, Feyrer F, Gingras M, Herbold B, et al. 2007. The collapse of pelagic fishes in the upper San Francisco Estuary: El colapso de los peces pelagicos en la cabecera del Estuario San Francisco. Fisheries. [accessed 2023 Sep 20];32(6):270–277. *https://doi.org/10.1577/1548-8446(2007)32[270:TCOPFI]2.0.CO;2*

Srinui K, Ohtsuka S. 2015. Supplementary description of three *Acartiella* species (Crustacea: Copepoda: Calanoida) from estuarine waters in Thailand. Species Divers. [accessed 2023 Sep 20];20(2):167–181. *https://doi.org/10.12782/sd.20.2.167*

Stan Development Team. 2021. Stan user's guide. Version 2.27. [accessed 2020 Oct 14]. Available from: *https://mc-stan.org/docs/2_24/stan-users-guide/index.html*

Tan Y, Huang L, Chen Q, Huang X. 2004. Seasonal variation in zooplankton composition and grazing impact on phytoplankton standing stock in the Pearl River Estuary, China. Continent Shelf Res. [accessed 2023 Sep 20];24(16):1949–1968. *https://doi.org/10.1016/j.csr.2004.06.018*

Tõnno I, Agasild H, Kõiv T, Freiberg R, Nõges P, Nõges T. 2016. Algal diet of small-bodied crustacean zooplankton in a cyanobacteria-dominated eutrophic lake. PLoS ONE. [accessed 2023 Sep 20];11(4):e0154526. *https://doi.org/10.1371/journal.pone.0154526*

Vehtari A, Gelman A, Gabry J. 2017. Practical Bayesian model evaluation using leave-one-out cross-validation and WAIC. Stat Comput. [accessed 2023 Sep 20];27(5):1413–1432. *https://doi.org/10.1007/s11222-016-9696-4*

Vroom J, Wegen M van der, Martyr-Koller RC, Lucas LV. 2017. What determines water temperature dynamics in the San Francisco Bay-Delta system? Water Resour Res. [accessed 2023 Sep 20];53(11):9901–9921. *https://doi.org/10.1002/2016WR020062*

Winder M, Jassby AD. 2011. Shifts in zooplankton community structure: implications for food web processes in the upper San Francisco Estuary. Estuaries Coasts. [accessed 2023 Sep 20];34(4):675–690. *https://doi.org/10.1007/s12237-010-9342-x*

Wood SN. 2011. Fast stable restricted maximum likelihood and marginal likelihood estimation of semiparametric generalized linear models. J Royal Stat Soc: Series B: Statistical Methodology. [accessed 2023 Sep 20];73(1):3–36. *https://doi.org/10.1111/j.1467-9868.2010.00749.x*

York JK, McManus GB, Kimmerer WJ, Slaughter AM, Ignoffo TR. 2014. Trophic links in the plankton in the low salinity zone of a large temperate estuary: top-down effects of introduced copepods. Estuaries Coasts. [accessed 2023 Sep 20];37(3):576–588. *https://doi.org/10.1007/s12237-013-9698-9*

Young MJ, Feyrer F, Stumpner PR, Larwood V, Patton O, Brown LR. 2021. Hydrodynamics drive pelagic communities and food web structure in a tidal environment. Intl Rev Hydrobiol. [accessed 2023 Sep 20];106(2):69–85. *https://doi.org/10.1002/iroh.202002063*

Zeug SC, Wiesenfeld J, Sellheim K, Brodsky A, Merz JE. 2019. Assessment of juvenile Chinook Salmon rearing habitat potential prior to species reintroduction. N Am J Fish Manag. [accessed 2023 Sep 20];39(4):762–777. *https://doi.org/10.1002/nafm.10309*